JANUARY 2021 M.Sc. in Electrical and Electronics Engineering BAHAULDDIN MKHAIBER RIJA

REPUBLIC OF TURKEY

GAZIANTEP UNIVERSITY

GRADUATE SCHOOL OF NATURAL & APPLIED SCIENCES

MICROCONTROLLER BASED AUTOMATIC POWER FACTOR CORRECTION FOR SINGLE-PHASE LOADS

M.Sc. THESIS

IN

ELECTRICAL AND ELECTRONICS ENGINEERING

BY

BAHAULDDIN MKHAIBER RIJA

JANUARY 2021

MICROCONTROLLER BASED AUTOMATIC POWER FACTOR CORRECTION FOR SINGLE-PHASE LOADS

M.Sc. Thesis

in

Electrical and Electronics Engineering

Gaziantep University

Supervisor

Assoc. Prof. Dr. Ahmet Mete VURAL

Co-Supervisor

Asst. Prof. Dr. Mahmut AYKAÇ

by

Bahaulddin Mkhaiber RIJA

January 2021

I hereby declare that all information in this document has been obtained and presented in accordance with academic rules and ethical conduct. I also declare that, as required by these rules and conduct, I have fully cited and referenced all material and results that are not original to this work.

Bahaulddin Mkhaiber RIJA

ABSTRACT

MICROCONTROLLER BASED AUTOMATIC POWER FACTOR CORRECTION FOR SINGLE-PHASE LOADS

RIJA, Bahaulddin Mkhaiber
M.Sc. in Electrical and Electronics Engineering
Supervisor: Assoc. Prof. Dr. Ahmet Mete VURAL
Co-Supervisor: Asst. Prof. Dr. Mahmut AYKAÇ
January 2021
69 pages

The reactive power is consumed by the loads which have lagging power factor. On the other hand, the reactive power is generated by the loads which have leading power factor. For both cases, the reactive power should be effectively monitored and controlled to increase the efficiency of the power systems. In this study, a microcontroller based automatic power factor correction system for single-phase loads is proposed. The designed system can correct the power factor of the loads with lagging or leading power factor by determining the required number of capacitor or inductor banks to be connected to the load in parallel. The designed system can also calculate and display many electrical parameters of the load. These parameters are rms voltage, rms current, real and reactive power, apparent power, power factor and power factor type. Arduino Mega 2560 microcontroller is used to perform signal measurements and calculations. The measurement ability of the designed system is tested by using resistive, inductive, and capacitive loads with two different sizes. The measurements results are compared with the measurements of a commercial digital power meter. A maximum measurement error less than 8.0% is attained. The power factor correction ability of the designed system is verified by using inductive and capacitive loads with two different sizes. The experiment results show that the designed system is able to improve the power factor of the load by making it close to unity for both lagging and leading loads.

Keywords: Reactive Power Compensation; Power Factor Correction; Lagging Load; Leading Load

ÖZET

TEK-FAZ YÜKLER İÇİN MİKRODENETLEYİCİ TABANLI OTOMATİK GÜÇ FAKTÖRÜ DÜZELTİLMESİ

RIJA, Bahaulddin Mkhaiber
Yüksek Lisans Tezi, Elektrik Elektronik Mühendisliği
Danışman: Doç. Dr. Ahmet Mete VURAL
İkinci Danışman: Dr. Öğr. Üyesi Mahmut AYKAÇ
Ocak 2021
69 Sayfa

Reaktif güç, geride güç faktörüne sahip yükler tarafından tüketilir. Diğer taraftan, reaktif güç, ileride güç faktörüne sahip yükler tarafından ise üretilir. Her iki durumda da güç sistemlerinin verimlerini artırmak için reaktif güç efektif bir şekilde izlenmeli ve denetlenmelidir. Bu çalışmada tek-faz yükler için mikrodenetleyici tabanlı otomatik olarak güç faktörü düzelten bir sistem önerilmiştir. Tasarlanan sistem yüke paralel bağlanacak kapasitör veya endüktör bankalarının sayısını tespit ederek güç faktörü geride veya ileride olan tek-faz yüklerin güç faktörünü düzeltebilir. Tasarlanan sistem aynı zamanda rms gerilim, rms akım, aktif ve reaktif güç, görünen güç, güç faktörü ve güç faktörü tipi gibi yüke ait birçok elektriksel parametreyi hesaplayıp gösterebilir. Arduino Mega 2560 mikrodenetleyicisi sinyal ölçümlerini ve hesaplamaları gerçekleştirmek için kullanımıştır. Tasarlanan sistemin ölçme yeteneği iki farklı büyüklüğe sahip resistif, endüktif ve kapasitif yükler kullanılarak test edilmiştir. Ölçüm sonuçları ticari bir sayısal güç metrenin ölçümleri ile karşılaştırılmıştır. En fazla %8.0'lik bir ölçüm hatası elde edilmiştir. Tasarlanan sistemin güç faktörü düzeltme yeteneği ise iki farklı büyüklüğe sahip endüktif ve kapasitif yükler kullanılarak doğrulanmıştır. Deney sonuçları tasarlanan sistemin güç faktörü geride ve ileride olan tek-faz yüklerin güç faktörünü bire yaklaştırarak iyileştirebildiğini göstermiştir.

Anahtar Kelimeler: Reaktif Güç Kompanzasyonu; Güç Faktörü Düzeltmesi; Geride Yük; İleride Yük

To My Parents, I am grateful to God for having parents like you. Your unconditional love and support made my every achievement possible.

ACKNOWLEDGEMENTS

In the name of Allah, the Merciful

I would like to take this opportunity to not extend my thanks and appreciation to everyone who supported me in making this project a success. Initially, I thank my supervisor, Assoc. Prof. Dr. Ahmet Mete Vural, for his comments and scientific advices that contributed to the success of this project.

I would also like to express my sincere appreciation to all the employees of the Department of Electrical and Electronics Engineering at Gaziantep University for their full support.

Finally, I would like to extend my thanks and gratitude to all my friends and family for their support to me, especially my parents and my wife, for their patience and continued support in all stages of my studies and life.

TABLE OF CONTENTS

LIST OF TABLES

Page

LIST OF FIGURES

Page

LIST OF ABBREVIATIONS

A	Ampere
AC	Alternating Current
APFC	Automatic Power Factor Correction
C	Capacitor
FACTS	Flexible AC Transmission Systems
H	Henry
I	Current
IC	Integrated Current
L	Inductance
LCD	Liquid Crystal Display
P	Power
PM	Power Meter
PCB	Printed Circuit Board
PF	Power Factor
Q	Reactive power
S	Apparent Power
SVC	Static Var Compensator
STATCOM	Static Synchronous Compensator
UF	Microfarad

V	Volt
VA	Volt-Ampere
VAR	Volt-Ampere Reactive
W	Watt

CHAPTER 1

INTRODUCTION

1.1 Introduction

The power factor (PF) is one of the critical performance indicators of the power quality in AC power systems [1, 2]. The PF of an electrical load is defined as the ratio between the real and apparent power of the load [1, 3]. The PF can be any value between 0 and 1. Ideally, the PF is equal to unity or 1, which means that a given load matches that of a pure resistance having voltage and current waveforms which are in phase [4]. This means that the real and apparent power of the load are equal to each other. In this situation, the load neither consumes nor delivers reactive power. On the other hand, if the PF is not unity, then the PF type can be either “lagging” or “leading”. Lagging PF means that the current waveform lags the voltage waveform by some angle. Instead, if the current waveform leads the voltage waveform, then the PF is said to be leading. For lagging PF loads, such as induction motors, power transformers, and lighting ballasts, the minimization of reactive power is very essential [3, 5]. Since the reactive power is the energy stored in inductive elements which continuously oscillates between the load and the source. This continuous oscillation causes an increase in the amount of current drawn by the load [2, 6]. If the reactive power is not minimized, a relatively higher amount of current will be drawn by the load, which makes imperative to use a relatively high cross-section of the conductors that increase the cost and losses of the distribution system [7].

Reactive power minimization is called as “Reactive Power Compensation” or “PF Correction”. This is a process that makes the PF of a load close to unity. With the PF correction, the load current is minimized without changing the real power consumed by the load [1, 8]. So, the load continues to make the same work by the drawn electrical energy with a relatively smaller amount of current when compared with the uncompensated case. Moreover, the minimum and maximum allowable limits of reactive power drawn from the system have been defined in regulations and the electric distribution companies give penalty to the industrial consumers for any violation of these limits. As a summary, the advantages of PF correction are the reduced system losses, increased load carrying capability of the conductors and the transformers, and improved voltage profile and system stability [9, 13].

Although there are some expensive solutions to handle the reactive power compensation function, the capacitors are still used in worldwide due to simplicity and economic reasons. When compared, the capacitors are much cheaper and easier to implement than Static Var Compensators (SVC), Static Synchronous Compensators (STATCOM), and active power filters [1, 3]. On the other hand, many papers proposed using a microcontroller to improve the PF of only lagging loads by adding parallel connected capacitor banks to the load [1, 9]. Arduino uno is generally used to improve only the lagging loads by using capacitor connections in parallel with the inductive loads [1, 6, 7]. Also, the Arduino uno is used to improve the PF in different loads by using inductor and capacitor banks [8]. Table1.1 show the comparison between the newest similar study and main contributions in this thesis

Table 1.1 Comparison between the newest similar study and main contributions in this thesis.

Previous study		Contribution
The Searches	Year	
Arduino Uno is generally used to improve only the lagging loads by using capacitor connections in parallel with the inductive loads [1, 6, 7]. The Arduino Uno is used to improve the PF in different loads	(2020, 2018, 2018). (2018).	The contribution of this work is to use the Arduino Mega 2560 microcontroller for automatic power factor correction (APFC) to improve the PF of both lagging and leading single-phase loads with different sizes. Not only the capacitor banks are used to improve the lagging loads but also the inductor banks are used to improve the PF of leading loads. Two different sizes in both load types, namely, inductive and

by using inductor and capacitor banks [8]. PIC18F452 microcontroller for the correction of the PF in constant level of load is proposed in [2].	(2019).	capacitive loads are used in this work to show the reliability of the designed hardware for performing APFC. The proposed APFC system is also able to calculate and display many electrical parameters of the load. Also, both power factor types are measured and corrected in proposed system. The proposed algorithm system can also function as a digital power meter measuring many electrical parameters (power factor, power, current , voltage ,resistor, inductor, and capacitor).

.

1.2 Related Works

In [14], Choudhury designed and implemented a small PF optimization device at low-cost. The design includes a small load and selects the appropriate capacitors for the load, and switches the suitable number of capacitors according to the load size.

In [15], Afridi designed and implemented a controller that controls the PF of a single-phase load and monitors the load by continuous measurements of the load. The study performs the automatic control of the PF using a smart controller where the controller estimates the value of the PF and compares it with the reference value.

In [16], sen Biswas optimized the PF with capacitors by observing the load PF continuously by a microcontroller. When the PF drops under a specific value, the controller calculates the capacitance value to be automatically added to the load by the relays which are also controlled by the controller.

In [17], Saha, et al. designed and developed the PF correction system using an AVR type microcontroller where the correction is done using a synchronous capacitor instead of a capacitor bank. This method includes continuous measurement and monitoring of the PF for inductive loads and generates the signal required to control the DC excitation for the synchronous capacitor to improve the PF.

In [18], the researchers used the single-phase capacitor banks to correct the PF. By this way, the capacitors reduced the reactive power consumption of the load, the losses are reduced, and the overall efficiency of the system is increased. The PF is corrected using an Arduino Uno controller.

In [19], Thai designed and simulated the PF automatically using an Arduino controller where the PF optimizer calculates the PF information by sensing the line voltage and the current. In the work, the phase angle of the load was adjusted and the load PF was calibrated.

In [20], Ranjan et al. have used the microcontroller unit to monitor the load and they considered it the cheapest way to compensate for the power factor in the delayed loads, the microcontroller calculates the power factor value and when it is less than one sends commands to the switching unit that will change the number of capacitors and connect them to the system to raise the power factor value

In [21], Raju et al. designed and implemented a PF correction device using one large transformer capacitor as a substitute for a capacitor bank using a two-way switch that controls the capacitor voltage and the capacitor offset current.

In [22], Stet et al. used a simulation software tool (EMTP- RV) to correct the PF by a compensation method in three-phase circuits using a three-phase delta-connected capacitor bank.

In [23], the authors used a PIC type microcontroller to correct the PF of both leading and lagging loads. After determining the zero crossover of the voltage and the current waveforms by means of a zero-crossing detector (ZCD) circuit, the capacitive bank or inductive bank is connected to the load to compensate the load PF.

In [24], Al-Thahab, et al. designed a PF correction system with an Arduino. There are sixteen levels for PF correction which are selected by a fuzzy logic approach. Four different capacitors are used. The fuzzy logic codes control the PF correction operation by turning on or off the capacitors.

1.3 The Place of the Work in the Literature

In this work, the PF improvement of both lagging and leading loads is prosed. The Arduino Mega 2560 microcontroller is programmed to decide how many capacitor or inductor banks are automatically connected to a single-phase load by means of relays to approach the load PF close to unity (0.98 lagging). Three different loads are considered in this work. These are resistive, inductive, and capacitive loads with two different sizes. The purpose of using resistive load is to verify the operation of the ZCD circuits. The designed APFC system can also measure and display many electrical parameters of the load on an LCD display. These parameters are rms voltage, rms current, real and reactive power, apparent power, PF, and PF type of the single-phase load. All the measurements are compared and verified with a commercial digital power meter (Reed R5000). The comparison results show that the measurement errors are relatively small with an error of less than 8.0%. On the other hand, it is experimentally verified that the designed APFC system can improve the PF by 39% for small inductive load, 52% for high inductive load, 12% for low capacitive load, and 29% for high capacitive load.

CHAPTER 2

LITERATURE REVIEW

2.1 Introduction

The PF is very important and considered as the core of effective, reliable and economical operation of the power systems. Therefore, it is of great importance in the electric power sector to control and monitor the PF of the loads to increase system efficiency. Hence there are many studies in the literature regarding the PF improvement of different types of loads. The following is a partial list of relevant work related to the PF correction.

2.2 Recent Papers about PF Correction

Mklakof et al. suggested a work to improve the energy efficiency in industrial networks using reversible AC motors with multilevel inverters [25].

Mansouri et al. utilized inverters to improve the PF and reduce the total harmonic distortion at the point of common coupling of the AC system [26]. The work was based on considering the use of converters that can be an alternative solution in correcting the PF of capacitive loads. The advantage is small size, high efficiency, and reduced cost.

Marcos-pastor et al. worked on the use of two interlocking digitally controlled boosting transformers that work on pulse width modulation (PWM) scheme to correct the PF [27]. Two transformers are separately controlled by an internal loop which is based on sliding mode approach which imposes a resistance behavior on each cell.

Marouani et al. covered in their work the improvement of the PF of a wind energy conversion system [28].

In their work, Moury et al. suggested a system consisting of multi-input transformers incorporating a PF improvement function with soft single-switch input modules for wind-solar hybrid systems in order to reduce the energy losses and costs [29].

Ravindran et al. proposed a method the improve the PF of low-cost reluctance motors [30].

Grey, in his work, used a synchronous motor for the purpose of correcting the PF using a fuzzy logic controller. The synchronous motor is adjusted by an independent human operator to provide the value of reactive power to achieve the required PF correction action [31].

Coman et al. designed a PF correction circuit that can be monitored and controlled through internet [32].

In the research of Hashmi et al., the stored energy is used to correct the PF [33]. The work involves connecting the storage devices connected to the inverter for the purpose of correcting PF by compensating for the reactive power where the solar energy is participated in the work.

In their work, Alberts et al. illustrated how renewable energy generation affects PF management and suggested the use of small-sized transformers which are capable of generating reactive power [34].

Beyamina et al. was suggested to use FPGA to perform a PF correction scheme [35].

Chandra et al. presented the correction of the PF and balanced the non-linear and unbalanced loads [36]. The method also regulates the voltage at the transformer end by implementing a new algorithm that controls an active three-phase shunt power filter based on DSP [36].

Chen et al. designed an active power filter in which a high-efficiency double inversion topology is used. The active power filter was installed to a power grid (MEA) in order to correct the PF, eliminate the harmonics, and reduce the effect of unbalanced loads [37].

Castro et al. used a FPGA based control system in fly-back converter [38]. It is shown that the FPGA allows simultaneous operation and high-performance control ability.

Gatta et al. presented an optimal power flow study for a distribution network. In the work, it is shown that it is able to control reactive power and improve the PF of a distribution network using MATPOWER [39].

Gonzalez-Santini et al. corrected the PF of a wireless charging system for electric cars [40]. A PF up to 0.987 was achieved in full-load and the voltage was regulated at 200 volts [40].

Wang et al. used in their work a fuzzy unit with a PLC industrial unit to improve the PF and automatically regulate the voltage in wind induction generator running at different speeds [41].

Allewar et al. worked to correct the PF in networks using photovoltaics systems connected to the grid [42]. The inverters was acted as a compensator for reactive power during low radiation at night or in the day and this helps the network in maintaining a stable voltage.

SM Rakiul Islam et al. considered the PF correction in smart homes using PF correction transformers without using individual bridges acting as reactive power sources in order to reduce the losses and increase stability [43].

Wanfeng Zhang et al. proposed a work to improve the PF using a predictive algorithm in smart built homes [44]. The work was verified with the application of DSP.

The aforementioned studies provided different techniques to improve the PF of different loads in different applications. In this thesis, the PF improvement of both lagging and leading loads is proposed. An Arduino Mega 2560 microcontroller is programmed to decide how many capacitor or inductor banks are automatically connected to a single-phase load by means of relays to approach the load PF close to unity (0.98 lagging).

CHAPTER 3

THE POWER FACTOR CORRECTION

3.1 The Power Factor

The power factor (PF) of a load is defined as the ratio of the active (real) power flowing into the load to the apparent power of the load. The active power is the power component that makes the actual work for the load, such as heating, motion, and lighting. On the other hand, the apparent power is obtained by multiplying the rms voltage and the rms current of the load. It is the combination of active and reactive power as shown in Figure 3.1. The reactive power is continuously exchanged between the source and the load with a zero-mean value. Because of this, the reactive power does not make any actual work such as heating or lighting. But the reactive power is necessary for some loads and devices for magnetic field production. Some examples for this load type are motors and transformers. The PF is a performance measure of the energy efficiency of an electrical load which is changing between 0 and 1. There are three types of PF; unity, lagging, and leading. The PF can also be defined as the cosine of the angle between the voltage and the current waveforms of the load. The unity or (one) PF means that the voltage and current waveforms of the load are in-phase, i.e., there is no phase angle difference between them. The PF of the resistive loads is unity. In this case, reactive power is neither consumed nor produced by the load. A large phase angle difference results in a poor PF. It means that the load requires relatively big amount of reactive power. Induction motors, power transformers, ballast lights, welders, and induction furnaces are such loads, usually have poor PF [17].

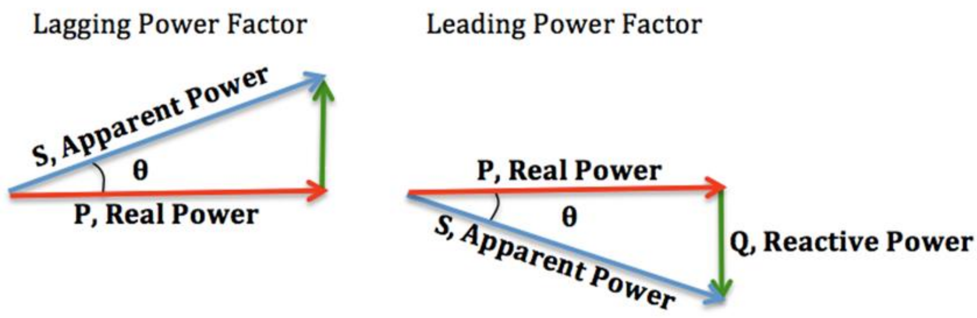

Figure 3.1 The power triangle of lagging and leading pf loads.

3.2 The Lagging and Leading PF

The lagging PF means that the current waveform of the load lags the voltage waveform by some degrees. In this case, the PF is less than 1 and the reactive power is said to be consumed or absorbed by the load. For lagging PF loads, the reactive power is assumed to be positive. Table 3.1 shows the typical PF values of some lagging loads. Oppositely, the leading PF means that the current waveform of the load leads the voltage waveform by some degrees. In this case, the PF is again less than 1 and the reactive power is said to be generated or delivered by the load. For leading PF loads, the reactive power is assumed to be negative. There are cases when the PF can be zero. In this case, the energy stored in the load at each cycle is fully reactive and no real power is absorbed by the load. An ideal inductor or an ideal capacitor are two examples for zero-PF case. Because of this property of the inductor and the capacitor, they can be used as source or sink for the reactive power in electrical systems. The utilization of inductors (or reactors) and capacitors for PF correction in electrical systems is known as “Reactive Power Correction/Compensation” [45, 46, 47].

The voltage of the load or system should be continuously monitored for stable operation of the power systems. The voltage and the reactive power are correlated with each other. Hence the reactive power control or the PF correction is essential on voltage stability of the power systems [48].

Table 3.1 Typical PF values of some lagging loads [49].

Load Type	Lagging PF	Voltage Dependence	
		P	Q
Large industrial motor	0.89	$V^{0.5}$	$V^{0.5}$
Small industrial motor	0.83	$V^{0.1}$	$V^{0.6}$
Refrigerator	0.84	$V^{0.8}$	$V^{2.5}$
Heat pup (cool/heat)	0.81/0.84	$V^{0.2}$	$V^{2.5}$
Dishwasher	0.99	$V^{1.8}$	$V^{3.5}$
Clothes washer	0.65	$V^{0.08}$	$V^{1.6}$
Clothes dryer	0.99	$V^{2.0}$	$V^{3.3}$
Color TV	0.77	$V^{2.0}$	$V^{5.0}$
Fluorescent lighting	0.90	$V^{1.0}$	$V^{3.0}$
Incandescent lighting	1.00	$V^{1.55}$	$-$
Rang, water or space heat	1.00	$V^{2.0}$	$-$

3.3 The PF in Various Circuits

In AC circuits, the shape of the voltage and current waveforms vary according to the load type. When the load is purely resistive as shown in Figure 3.2, the voltage and current waveforms are in-phase as shown in Figure 3.3. It means that the phase angle between the voltage and the current waveforms is zero. When the load is inductive as shown in Figure 3.4, the PF is said to be lagging and the load consumes reactive power. In this case, the voltage and current waveforms of the load are not in-phase. The current waveform lags the voltage waveform by some degrees as shown in Figure 3.5. When the load is capacitive as shown in Figure 3.6, the PF is said to be leading and the load generates reactive power. In this case, the voltage and current waveforms of the load are not in-phase. The current waveform leads the voltage waveform by some degrees as shown in Figure 3.7. [50].

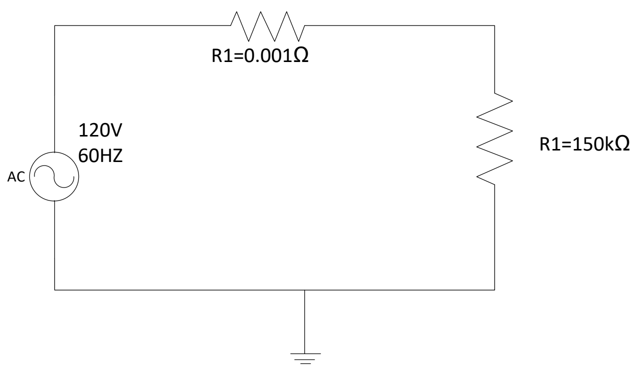

Figure 3.2 A purely resistive circuit.

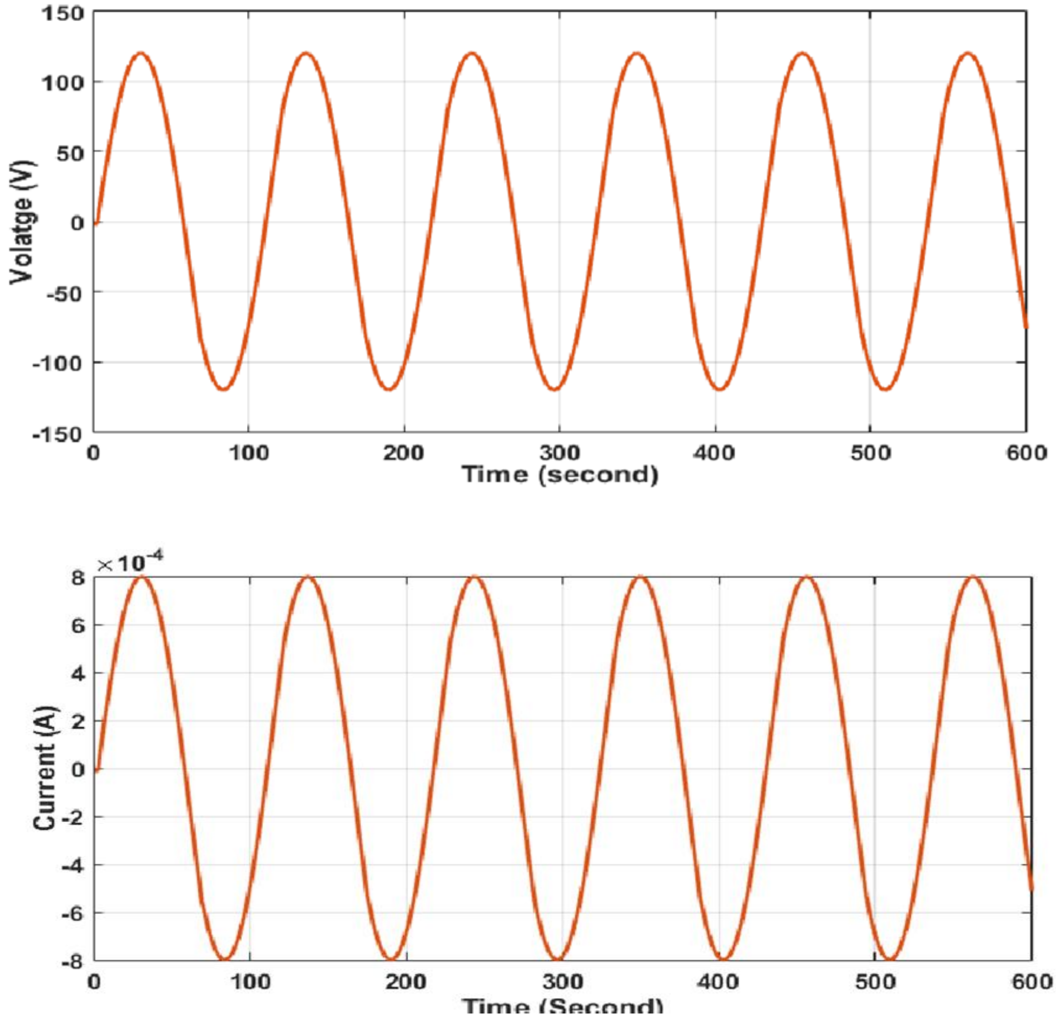

Figure 3.3 The voltage and current waveforms of a pure resistive load.

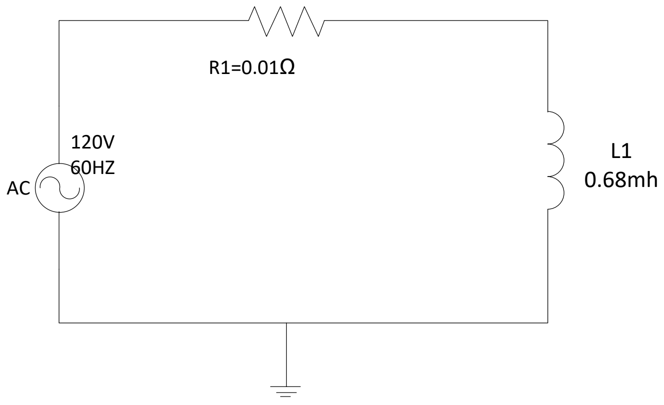

Figure 3.4 An inductive circuit.

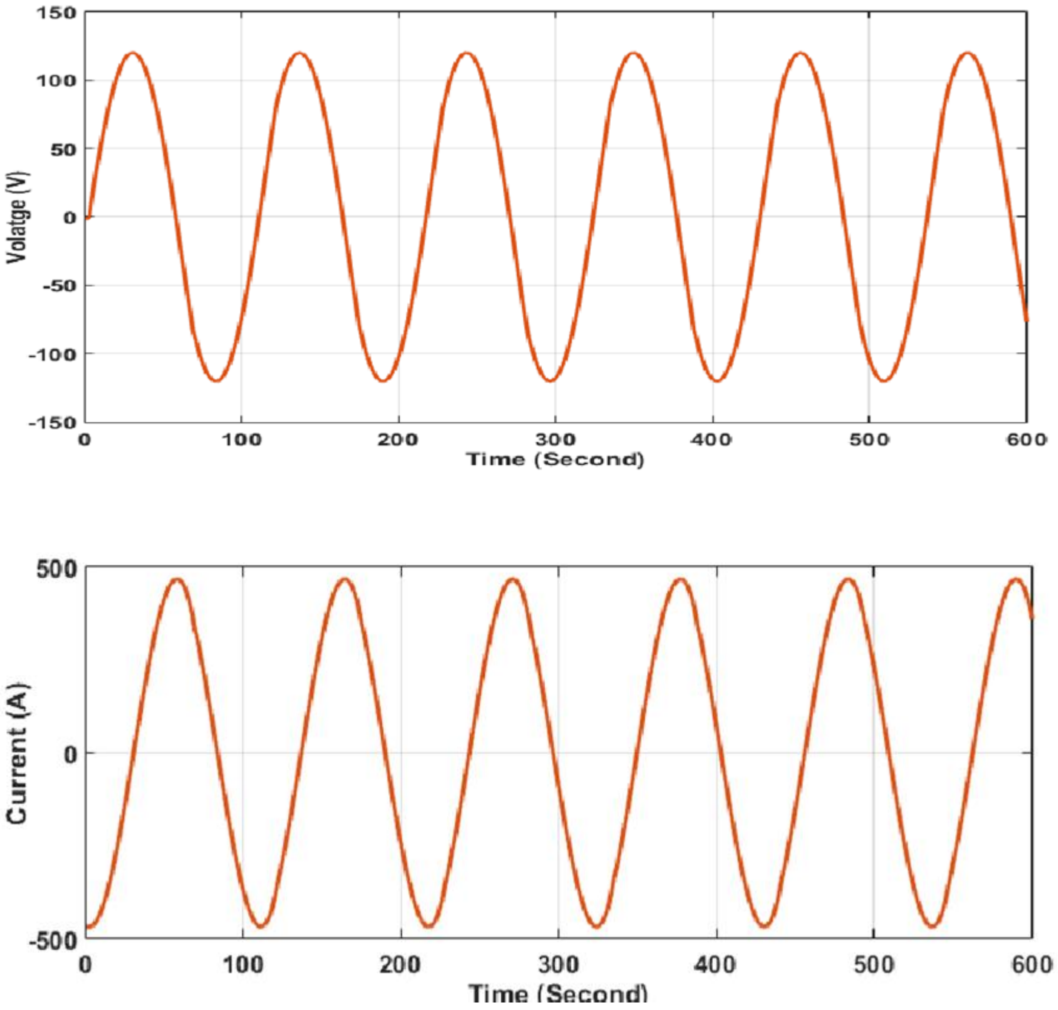

Figure 3.5 The voltage and current waveforms of an inductive load.

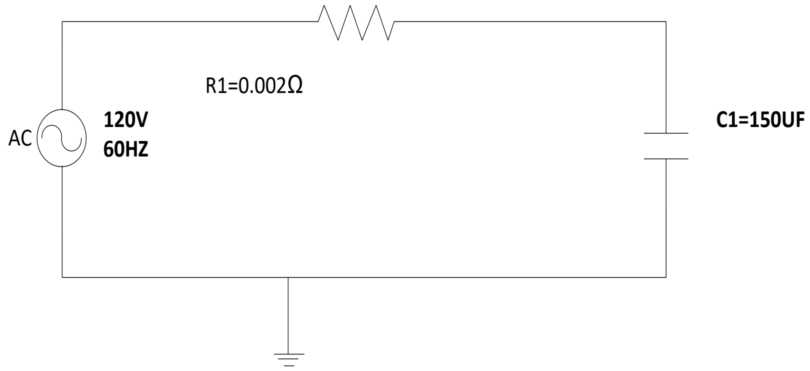

Figure 3.6 A capacitive circuit.

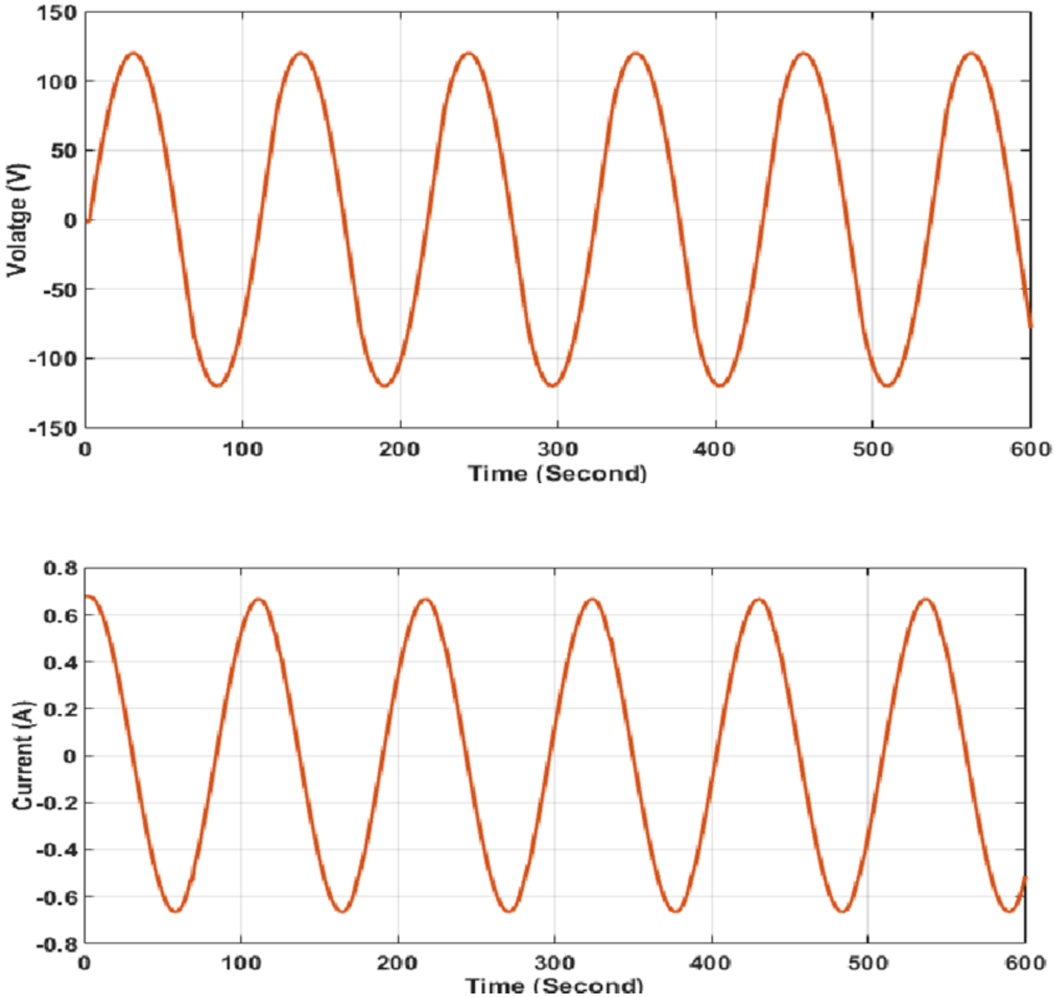

Figure 3.7 The voltage and current waveforms of a capacitive load.

3.4 Capacitor

A capacitor (condenser) consists of two conducting surfaces which are separated by a dielectric insulation medium. The surfaces may be in circular, rectangular, spherical, or cylindrical form. The positive end of the supply is connected to one plate called anode and the other end (negative or neutral) is connected to the other plate (cathode) of the capacitor. The capacitor stores the electrical energy in the form of electric field [51]. The capacitor is able to generate a reactive power which can be expressed as,

$$Q = \frac{V^2}{X_c} \tag{3.1}$$

where, Q is the reactive power of the capacitor (VAR), V is the rms voltage of the capacitor (V), and $X_c = 1/2\pi f C$ is the capacitive reactance of the capacitor (Ω). Shunt capacitors are used in a number of sizes in the utility. For PF correction, Shunt condensers were first used in the mid-1910s. Oil was used as the dielectric for early condensers. Their use was limited at that time, due to their weight and high cost. By using inexpensive dielectric materials and other developments in condenser design in the 1930s, price and size decreased significantly. Since the late 1930s, shunt condensers had been used to a huge degree. They still provide today a very cost-effective solution to produce reactive power. The major advantages of shunt condensers are cheap price and installation and service flexibility. They are also easy to use in different parts of the electrical systems to boost transmission and distribution performance. The key downside of the shunt condenser is such that the amount of reactive power is the function of square of the condenser voltage as shown in Equation (3.1). So under low voltage conditions, the generated reactive power by the condenser will be small where it is needed at most [49].

3.5 Inductor

An inductor can be formed by a conductive wire wrapped around a coil. The inductors are classified according to the type of the core used on which the wire is wound. Usually this core can be air, or any magnetic material such as iron. The inductors are used in many applications, such as filters. The inductors can also be used as a circuit element that consumes reactive power. Hence an inductor can be participated in reactive power compensation scheme by connecting it in parallel to the load. The reactive power consumed by an inductor is expressed as,

$$Q = \frac{V^2}{X_L} \tag{3.2}$$

where, Q is the reactive power of the inductor (VAR), V is the rms voltage of the inductor (V), and $X_L = 2\pi f L$ is the inductive reactance of the inductor (Ω) [52].

3.6 PF Correction

Correcting the PF is the process of reducing lagging or leading current in AC circuits and approaching the PF close to unity by providing or absorbing the required amount of reactive power to the load. This function is realized either by an inductor (or inductor/reactor banks) or a capacitor (or capacitor banks). If the load has a lagging PF, the reactive power required by the load is met by a capacitor. On the other hand, if the load has a leading PF, the excess amount of reactive power produced by the load is allowed to be consumed by an inductor. In either case, the capacitor or inductor is connected to the load in parallel, i.e., they see the same voltage as the load. In PF correction, usually, not all the amount of reactive power is consumed/supplied by the inductor/capacitor. Instead, the reactive power consumption/supply is shared between the inductor/capacitor and the utility to make the PF close to unity [50]. Generally, there are three types of PF correction methods: Active, passive, and synchronous.

3.6.1 Active PF Correction

It is the best type of PF correction methods but it is an expensive solution. This method can effectively perform an automatized PF correction action with high speed and good flexibility [50]. In this method, FACTS (Flexible AC Transmission Systems) devices such as SVC [53, 54], or STATCOM [55, 56], are used as shown in Figure 3.8 and 3.9, respectively. These devices are power electronic based and hence their control loops are very fast so that they can efficiently produce or consume the required amount of reactive power. These devices give satisfactory control performance for the correction of the PF of the loads.

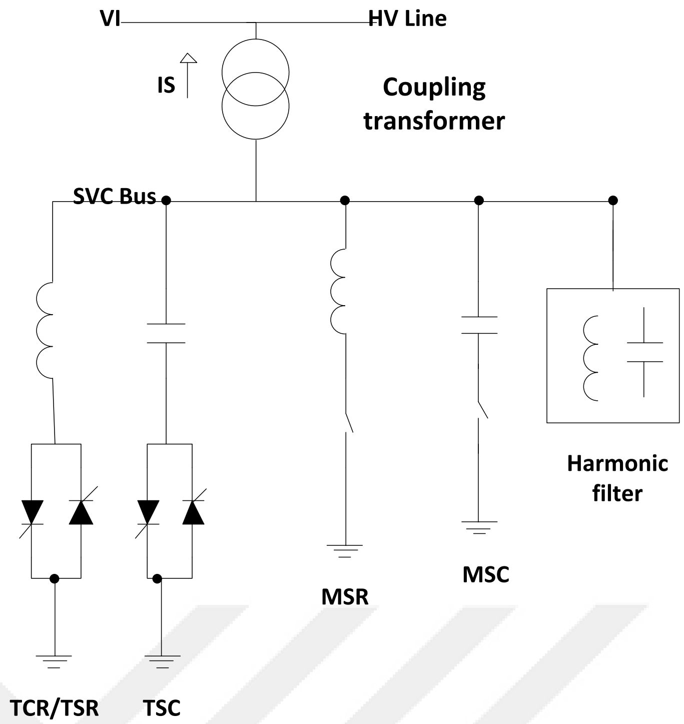

Figure 3.8 Basic SVC configuration [57].

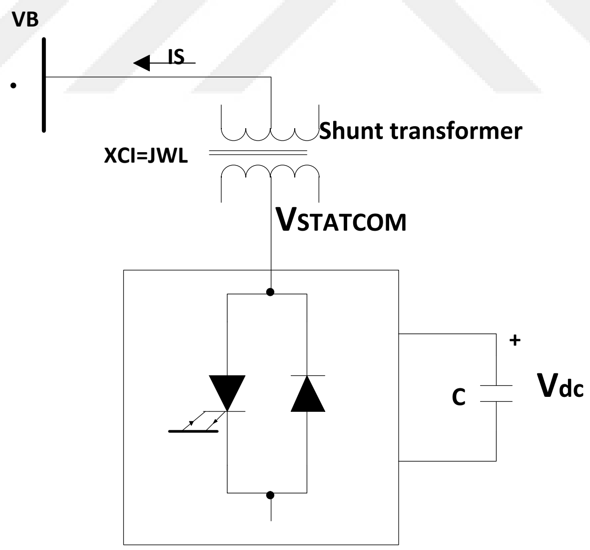

Figure 3.9 Basic STATCOM configuration [57].

3.6.2 Passive PF Correction

This method is more economical than active PF correction method. In this method, as shown in Figure 3.10, the required amount of lagging or leading reactive power is obtained by connecting the pre-calculated amount of reactor or capacitor banks to the load. This method is also automatized but gives slower response than the active PF correction method. Another disadvantage of this method is that since the capacitor or reactor banks are mechanically switched, the maintenance requirement is high [50, 58, 59].

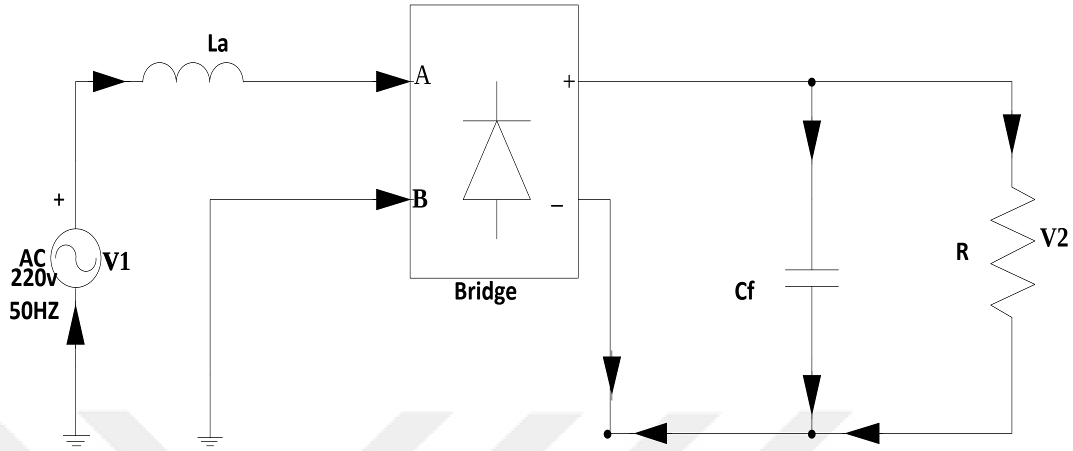

Figure 3.10 Passive PF correction [60].

3.6.3 Synchronous PF Correction

This method is an old method and not applied frequently nowadays because of the frequent maintenance requirement. In this approach, as shown in Figure 3.11, a free-rotating synchronous motor (without a mechanical load) is connected in parallel to the electrical load of which the PF is to be corrected. By controlling the field excitation of the synchronous motor, the required amount of reactive power for both lagging and leading loads can be dynamically obtained [61,62, 63].

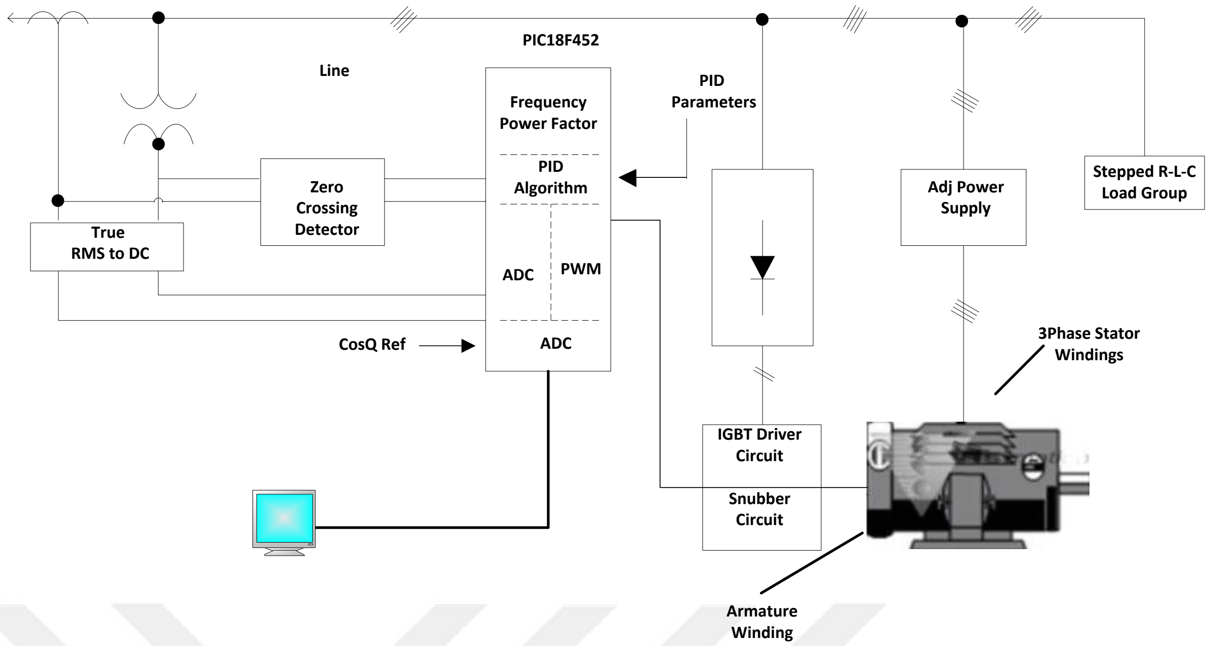

Figure 3.11 Synchronous PF correction [64].

3.7 Disadvantages of Low PF Operation

The PF has an important and effective role in the AC circuits and has a direct impact on the loss minimization and the efficiency of the system. There is a relationship between the PF and the real power in both single and three-phase AC circuits. This relationship in a single-phase AC circuit is given as,

$$P = VIcos\theta \tag{3.3}$$

where, P is the active power (W), V is the rms voltage (V), I is the rms current (A), and $cos\theta$ is the PF of the single-phase load. This relationship in a three-phase AC circuit is given as,

$$P = \sqrt{3}\, VI\, cos\theta \tag{3.4}$$

where, P is the three-phase active power (W), V is the rms line-to-line voltage (V), I is the rms line current (A), and $cos\theta$ is the PF of the three-phase load. As seen in Equation (3.3) and (3.4), a low PF value reduces the active power consumption of the load although the apparent power of the load does not change [50].

3.8 Benefits of PF Correction

There are many benefits of PF correction in electrical utility systems. These can be listed as follows [65]:

1. Abolishing the PF penalty of the companies.
2. Reduced electrical losses.
3. Expanding the load carrying capability of the transformers and cables.
4. Improving the voltage regulation by reducing the voltage drops on the transmission/distribution system.
5. Increasing the overall system efficiency.

3.9 Strategies for PF Correction

There are different methods to improve the PF in industrial plant. These are individual compensation, group compensation, and plant compensation [49]. These strategies are schematically summarized in Figure 3.12. In individual compensation, each lagging load such as motor is compensated by a shunt connected capacitor or capacitor banks. So, if the motor is inactive, there is no need for PF correction. In group compensation, more than one lagging loads are compensated by a shunt connected capacitor or capacitor banks. It is not mattering how many motors are running at one time. The reactive power compensation relay chooses the necessary number of capacitors to be connected. In plant compensation, the compensation is applied at the medium voltage side of the transformer. The phase angle between the voltage and the current of the plant is continuously measured by the reactive power compensation relay to decide the number of capacitors to be connected [65].

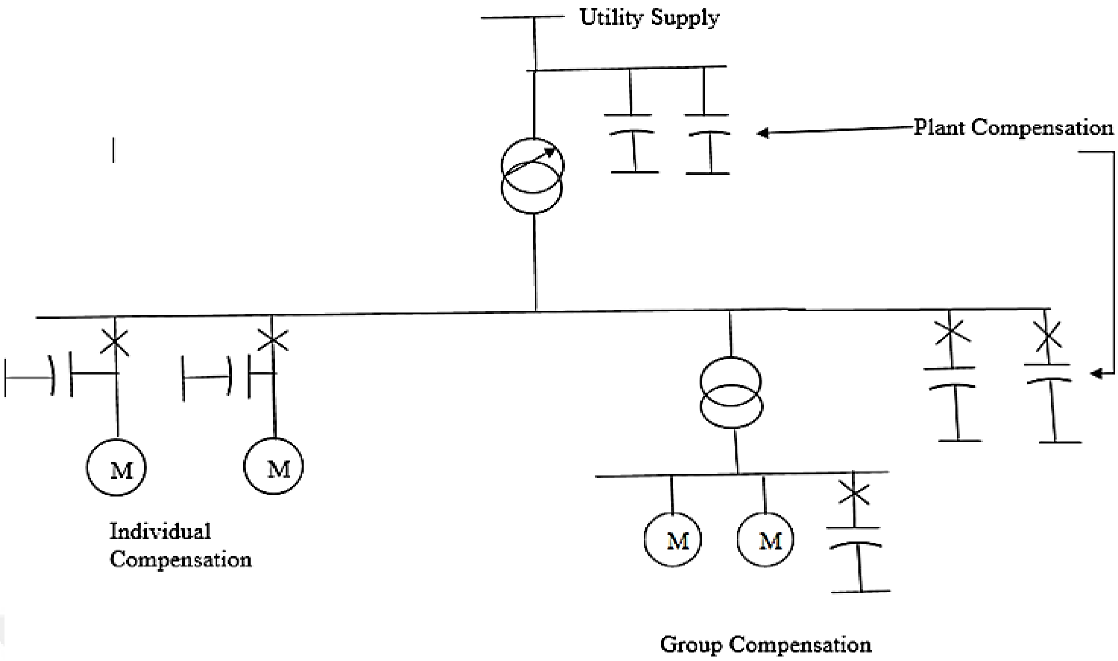

Figure 3.12 PF Correction in industrial plants [49].

3.10 Demerits of Capacitive PF Compensation

3.10.1 Capacitor Selection

In the PF correction process, there are defects that must be taken into account. The correction of the fixed PF should not be more than 80% of the excitation (magnetizing) current of the motor. As the correction of the PF to a very high value can cause several problems. One problem is the equipment failure and damage in the motor and capacitors. There is a big variety in the current rating of the induction motors which greatly varies from one design to another. The proportion of the excitation current is always higher than 20% of the load current of the motor and sometimes it can reach up to 60% of the rated current of the motor. There are standard application tables in the literature to show the technicians and engineers the necessary amount of the capacitors to be added. However, these tables assume the lowest number of capacitors according to the magnitude of the excitation current. This means that the correction is often less than the half value to be reached. There are two approved methods through electrical calculation programs to calculate the correct value of the reactive power for the motor. The first method requires knowing the value of the excitation current of the motor and if it can be obtained this is the best way. If the value of the excitation current cannot be obtained, we use a second method that depends on the value of the half-load PF and the motor's efficiency [59].

3.10.2 Supply Harmonics

Harmonics occur due to non-linear loads in the power systems. Power electronic converters and the saturated transformers are some typical examples to non-linear load. The current waveforms of the non-linear loads are distorted which are not perfectly sinusoidal. These distorted current waveforms have low order harmonics such as 3,5,7 or more. These waveforms can also distort the voltage waveforms in the power systems. The low order harmonics cause higher currents to flow to the capacitors and this situation leads to an increase in the temperature of the capacitors. This case reduces the lifespan of the capacitors. There are passive and active power filter systems as an effective solution to reduce the harmonics. Although these methods are efficient, they are relatively expensive. Alternatively, an intermittent reactor(s) can be installed together with the PF correction capacitors. By this way, the effective capacity over the supply frequency is reduced and the effects of fifth or higher harmonics are reduced. The reactors designed in this way make the necessary induction correction for higher frequency harmonics [59].

3.10.3 Detuning Reactor

Passive filters protect the capacitors from the harmonic amplification caused by resonance and work against the current flow that causes damage to the capacitors and circuit breakers. These reactors are connected with the capacitors which in turn will increase the capacitor's resistance to harmonics that greatly reduces the harmonic distortion in the power network. With this solution, the thermal pressure caused by the harmonics is reduced and hence the life of the capacitors is increased. The detuning reactor is shown in Figure 3.13. The PF correction leads to an echo between the capacitor and the source, so the resonance effect will be minimal if the fault current is high in the supply. However, the load may be very inductive in the rural installations and the resonance can be very severe which causes significant damage to the equipment. The size of the voltage depends mainly on the value of the reactive power of the circuit, which is the function of loading the circuit. There are steps that can be applied in order to reduce the problem of resonance of the supply. For light loads, the level of PF correction is reduced, which in turn causes the losses to reduce in the supply. The harmonics due to PF correction cannot be corrected on the circuits that draw distorted waveforms. The PF correction cannot be efficiently achieved for distorted supplies but the harmonics can be reduced by designing a suitable equipment such as active rectifier, adding electronic PF correction adapters or LCR filters which restores the waveform to the normal state [59, 66, 67].

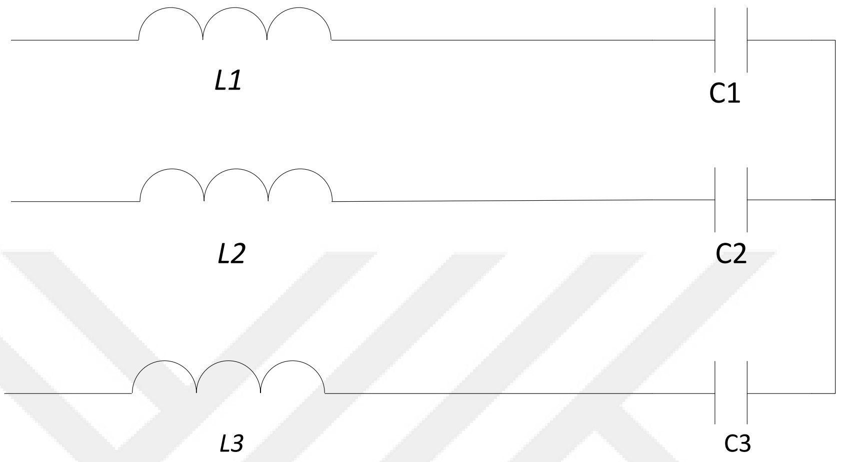

Figure 3.13 Detuning reactor.

CHAPTER 4

AUTOMATIC POWER FACTOR CORRECTION CIRCUIT

4.1 Hardware Design

The schematic block diagram of the proposed automatic PF correction circuit is shown in Figure 4.1. This circuit determines the necessary number of capacitor or inductor banks to be connected to the load to improve the PF by measurements. This circuit can also display many electrical parameters of the load, such as, rms voltage, rms current, real/reactive power, apparent power, PF, and PF type. These parameters are shown on a 2004A LCD display. At first, the voltage and current waveforms of the load connected to the 220V single-phase source are sensed by using an ASL 150212 voltage transformer and a ZMCT 103C current transformer, respectively. Then the voltage and current signals are sent to ZCD circuits. The ZCD circuit is used in this design to convert the voltage/current sinusoidal waveforms into the square waveforms. The corresponding sinusoidal signal is synchronized with the square waveform such that both signals pass through their zero points at the same time. The two produced square signals are then sent to an exclusive OR (XOR 3040) logic gate. This logic gate generates logic-1 if both inputs are different, otherwise it generates logic-0. By this way, the XOR logic gate generates a continuous pulse signal at its output. The width of this pulse is proportional to the phase angle difference between the voltage and current waveforms of the load. The output of the XOR logic gate is connected to one I/O pin of the Arduino Mega 2560 microcontroller. The microcontroller measures the width of the pulse that the XOR logic gate generates. This time duration is converted to an information about the phase angle difference. At this step, also, the PF type (unity, lagging, leading) is also detected ,When the pulse arrived to the Arduino is from the XOR (Logic-0), this means that the load is resistive, but when the pulse arrived to the Arduino is from the XOR (Logic-1), this means that both input signals are different, the Arduino works to interrupt and checks the voltage and current pins if the first positive pulse comes from The current means that the current is leading the voltage (Leading load), and if the first positive impulse comes from the voltage, this means that the voltage is leading the current (lags load). The PF calculation and the detection of the PF type are implemented in the microcontroller with a program written in C language. The codes of this program are given in the Appendix. After the PF calculation and PF type detection, the microcontroller decides the required number of capacitor or inductor banks to be connected in parallel with load to correct the PF of the load. Each capacitor/inductor bank is connected to the load in parallel with a relay for each. So, the required relays are triggered by the microcontroller to connect the required capacitor/inductor usage to the load.

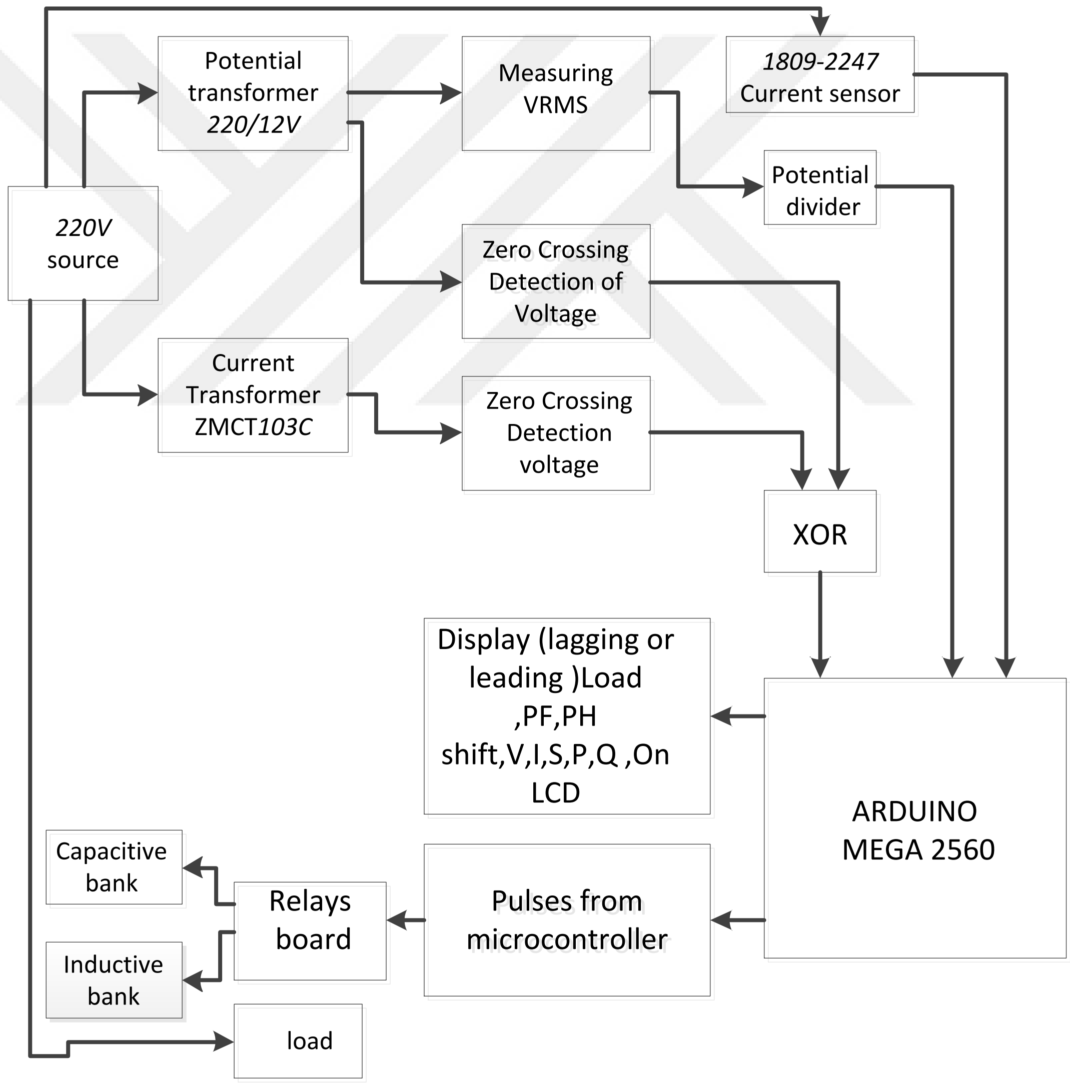

Figure 4.1 The block diagram of the proposed automatic pf correction circuit.

The hardware of the automatic PF correction circuit is shown in Figure 4.2. The PCB board is designed according to the scheme drawn on the Proteus program. The PCB board consists of the voltage transformer, current transformer, ZCD circuits, Arduino Mega 2560 microcontroller, LCD, relays, and capacitor/inductor banks. Each part is checked by means of a multimeter to avoid any accidental shortening. The program is written in the computer and then uploaded to the microcontroller by USB connection. The capacitor banks consist of 0.5uF,1uF1.5uF,2.5uF, and 5uF capacitors. The inductor banks consist of 0.68H,0.73H,1.01H, and 2.91H inductors.

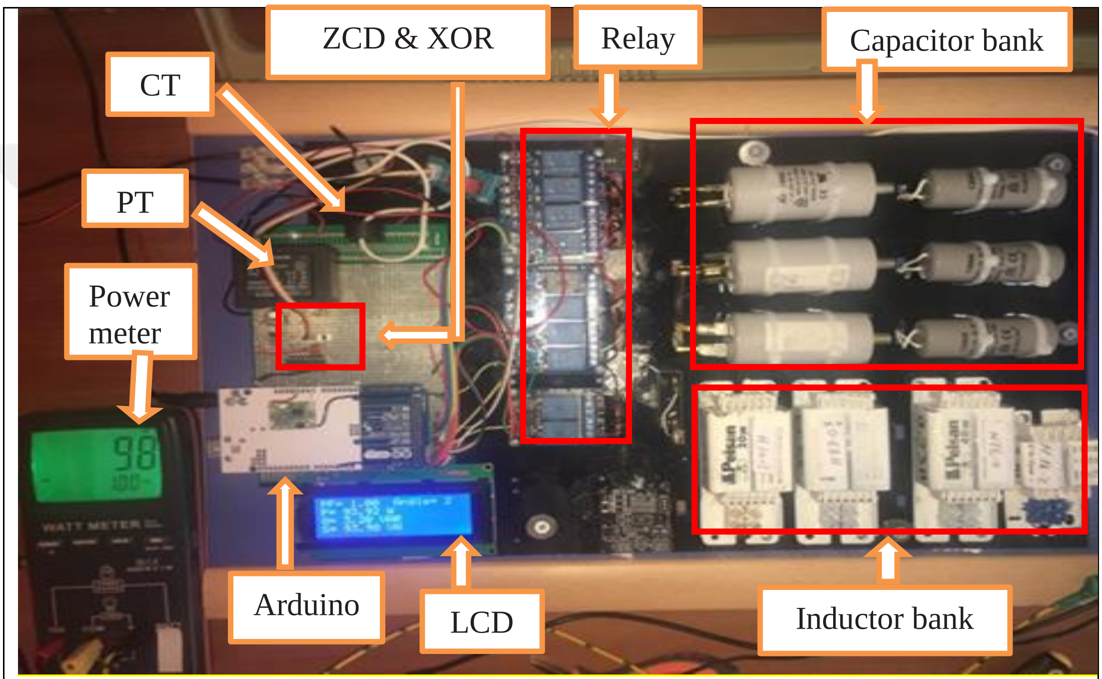

Figure 4.2 Hardware of the automatic PF correction circuit.

4.1.1 Microcontroller

A microcontroller is a control and communication unit which interferes with diverse modules and peripherals in the same circuit. A microcontroller is able to merge various functions together by using different units. In this work, Arduino Mega 2560 microcontroller board Rev3 is used as shown in Figure 4.3. This microcontroller is based on the ATmega2560 with 54 digital input/output pins, 16 analog inputs, 4 serial ports, and a 16 MHz crystal oscillator. It also has a USB connection, an ICSP header, a power jack, and a reset button. The 15 pins can be used as PWM outputs. Arduino

Mega 2560 microcontroller is supplied from a 5V USB port of a computer or an AC-DC converter. The flash memory capacity is 256 Kb, the SRAM capacity is 8 Kb, and the EEPROM capacity is 4 Kb. All 54 pins on Arduino Mega 2560 can be used as input or output by using commands such as pin Mode (), digital Write () and digital Read (). It also has 16 analog input pins and these pins have a resolution of 10 bits. Arduino Mega 2560 can easily communicate with computers, other Arduino's or other microcontrollers. Arduino Mega 2560 can be programmed with a USB connection using the free and open-source Arduino IDE, thanks to its built-in programmer. At the same time, the microcontroller in the card can be programmed with the Cytron USB ICSP PIC programmer head without using the internal programmer. In this work, Arduino Mega microcontroller 2560 is programmed with C software which is downloaded to the Arduino Mega 2560 board via a USB cable. This program calculates the phase angle difference between the voltage and the current waveforms of the load by reading the output of XOR logic gate. Second part of this program is used to read the measured voltage and current values of the load and it calculates the electrical parameters of the load such as rms voltage, rms current, real/reactive power, apparent power, PF, and PF type [67].

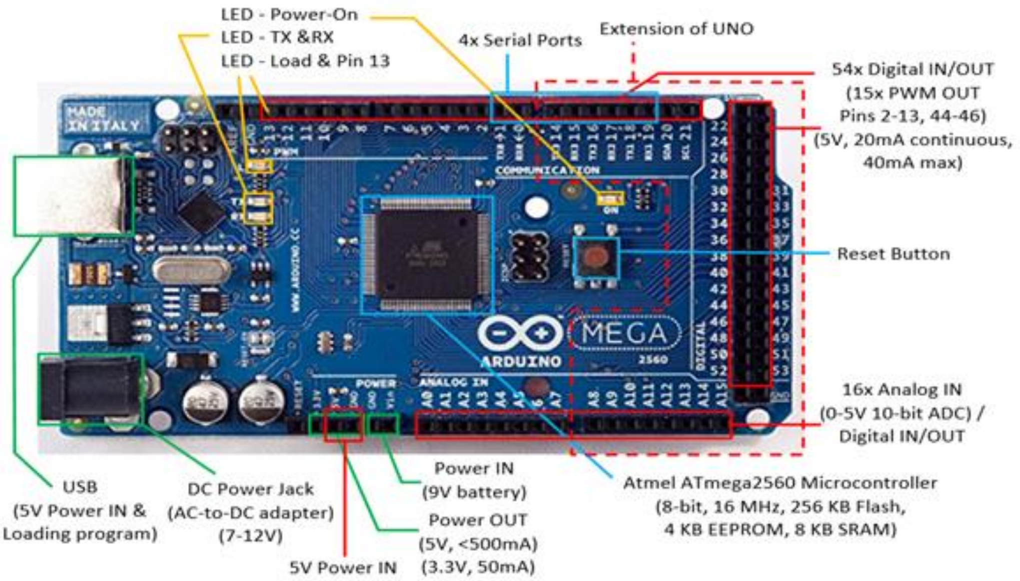

Figure 4.3 Arduino mega 2560 pin description [68].

4.1.2 Zero-Crossing Detector

The zero-crossing detector (ZCD) is an electronic circuit that converts the sine wave into a square wave which is in-phase with the sine wave. A ZCD circuit can be made from an op-amp and additional components as shown in Figure 4.4. The negative and the positive input of the op-amp is connected the sinusoidal signal source and the ground, respectively. As seen in Figure 4.4, the output signal is a square wave which is in-phase with the input sinusoidal signal. The output voltage waveform shows the time and direction of the zero crossing of the input signal. If the input voltage signal is low-frequency, the output voltage will be less rapid in switching from one saturation point to another. But, if there is noise between the input nodes, the output will oscillate between negative and positive saturation voltage [17]. In this study, two ZCD circuits are used, i.e., one is for the current waveform of the load and the other one is for the voltage waveform of the load. Figure 4.5 shows the LM324 op-amp which is used to design ZCD circuits in this work.

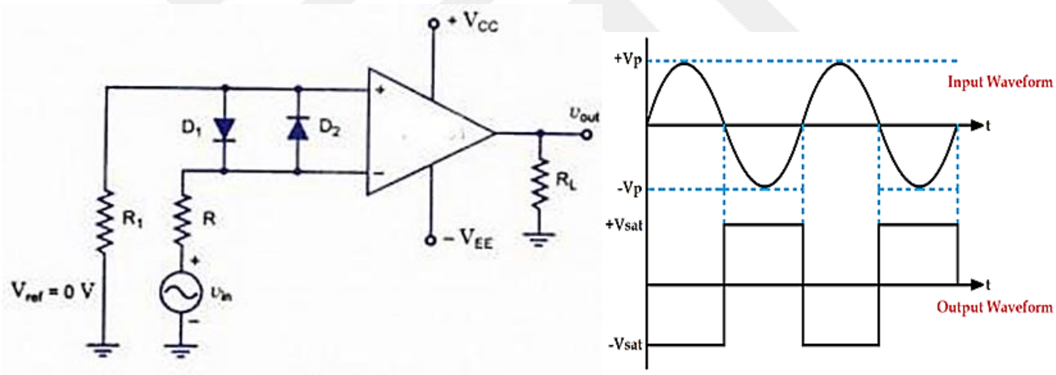

Figure 4.4 A typical ZCD circuit and output waveform.

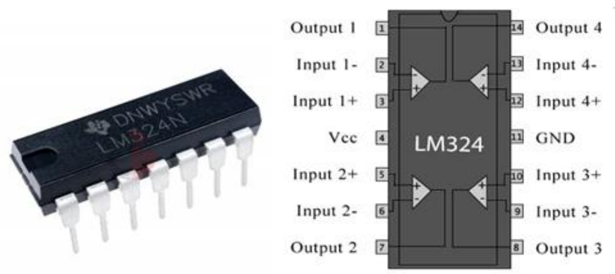

Figure 4.5 LM324 IC and pin diagram.

4.1.3 Voltage Transformer

The voltage (or potential) transformer (ASL 150212) is an instrument transformer used to measure the load voltage by reducing it a suitable value. In the design, a voltage transformer with a ratio of 230V/12V is used as shown in Figure 4.6. The voltage transformer consists of a primary and a secondary winding which are all wound on a ferrous core consisting of laminated sheets to reduce eddy current losses.

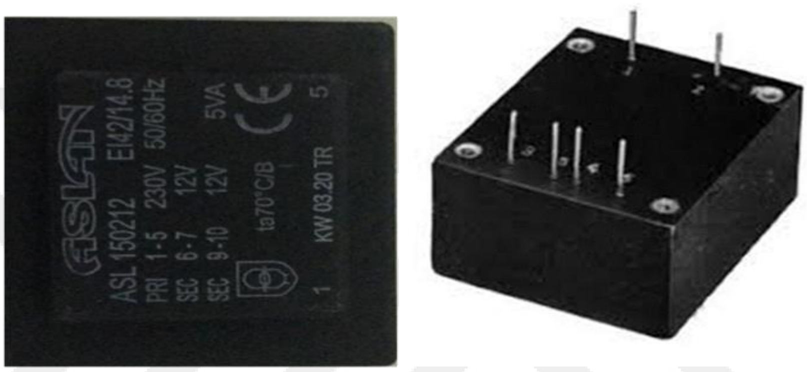

Figure 4.6 The voltage transformer used in this work.

4.1.4 Current Transformer

The current transformer (ZMCT 103C) is another type of the instrument transformers used to convert the AC current into a current value as shown in Figure 4.7. By this way, it becomes possible to measure AC currents for control and protection purposes. The current transformer consists of a primary winding, a secondary winding, and a magnetic core usually made from a silicon steel ring. The primary coil consists of a single rotating wire with a large cross-section while the secondary coil consists of a large number of windings. When the AC current to be measured passes through the primary coil, a magnetic field in the magnetic core is produced and this magnetic field induces an AC voltage in the secondary coil. This current signal is then converted to a voltage signal by using a resistance. The design is made such that the secondary current becomes linearly proportional to the primary current.

Figure 4.7 The current transformer used in this work.

4.1.5 Relays and Driver

The relay unit is an electromagnetic relay that is controlled by the digital output pins of the microcontroller. In this work, the relay unit is used as a controllable switch to connect the required capacitor or inductor bank to the load in parallel to improve the PF. The output of the microcontroller switches to the driver and switches the relay from the open position (OFF) to the closed position (ON). By this action, connecting the required element to the main circuit is possible. The rest of the relays will remain in the open position. The relays board with their drivers used in this work are shown in Figure 4.8. The schematic diagram of the relay module is shown in Figure 4.9. The control circuit of the relay needs a low voltage. In this work, the relays are operated with 5 V DC. At the beginning, before compensation, all the relays are in the normally open state where the relays are controlled individually through the relay header and the 5 V DC supply. When the current passes through the solenoid, a magnetic field is generated, forcing the solenoid to move upwards and closes the contact.

Figure 4.8 Relays board with their drivers used in this work.

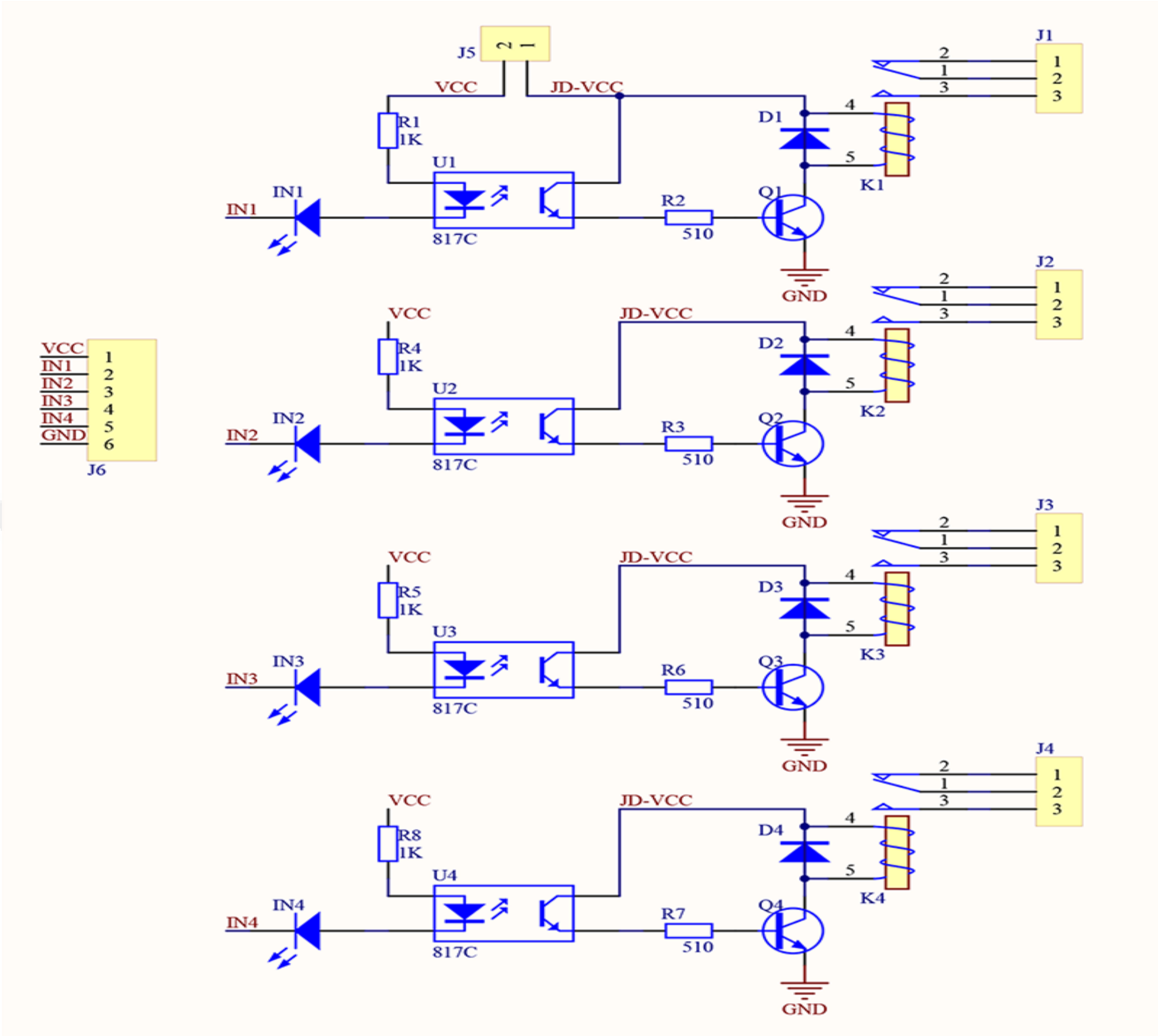

Figure 4.9 Schematic diagram of the relay module.

4.1.6 LCD

In this work, a 20x4 LCD, as shown in Figure 4.10. is used to display the calculated electrical parameters of the load. This LCD has 20 columns and 4 lines. The basic structure of the LCD screen is two patterned glass panels. The space between these panels is filled with liquid crystal material and the thickness of the glass varies ranging from 0 .70 mm to 1.1 mm where a spiral staircase is formed to distinguish the light by placing liquid crystal particles between the glass panels. LCD screen is also called optical switches which acts as an interface between the electronic circuits to give an optical output.

Figure 4.10 The 20x4 LCD used in this work.

4.1.7 Adapter Power Supply

The adapter is a power transformer that is lightweight and compact and has the ability to provide a DC power source for any portable electrical device, and it varies between them according to the device and the voltage value to be converted to. It processes the power supply from an external AC source to a DC source.

The internal components of the adapter in general are a charge and discharge circuit, transistors, capacitors, and resistors that perform manipulations on the supply of energy taken from an external source to convert it to the required value, in our work we used an electrical power transformer that converts the voltage from (*220V,50HZ) AC to (12V) DC*, as shown in the Figure 4.11 [69].

Figure 4.11 Adapter power supply 220/12V ,1A.

4.2 Software Design

The development programs are free and open-source for Arduino Mega 2560 microcontroller. The programming language is C. In this work, the codes are written in C. There are several functions in the programming stage of this microcontroller. On the other hand, the digital pins on the board can be used as inputs that can be programmed for general purpose via the commands pin Mode (), digital Write (), and digital Read (). Each of these pins contains an internal pull resistance that can be controlled by using digital Writing () (w/a HIGH or LOW). When the pin is used as an input, this type of program is called (sketches) after which a semicolon must be placed at the end of all command lines. One of the inputs of the Arduino Mega 2560 microcontroller is related with the phase angle difference between the voltage and the current waveforms of the load. These valu es are read by the microcontroller using the function "pulseIn (pin, value, timeout)". The PF of the load is then calculated by using the following equation,

$$PF = cos\,\theta \tag{4.1}$$

where, θ is the phase angle difference between voltage and current waveforms of the load. Based on voltage and current measurements as well as PF calculation, apparent power, real power, and reactive power of the load are calculated by the following equations,

$$S = V * I \tag{4.2}$$

$$P = S * PF \tag{4.3}$$

$$\mathrm{Q} = \sqrt{S^2 - P^2} \tag{4.4}$$

where, S is the apparent power (VA) of the load, V is the rms voltage of the load (Volt), I is the rms current of the load (A), P is the real power of the load (W), and Q is the reactive power of the load (VAR), respectively. The PF of the load can be unity, lagging, or leading based on the load type. If the load is resistive, then the PF becomes unity and no action is needed from the microcontroller. Only the electrical parameters mentioned before are calculated and shown on the LCD display. If the load is inductive, the PF becomes lagging. In this case, the microcontroller calculates the size of the capacitor banks to be connected in parallel with the load to raise the PF close to unity. This is achieved by controlling the relays between the load and the capacitors. If the load is capacitive, the PF becomes leading. In that case, the microcontroller calculates the size of the inductor banks to be connected in parallel with the load raise the PF close to unity. This task is achieved by controlling the relays between the load and the inductors. The following steps are executed to calculate the required capacitance or inductance for the compensation,

Step 1: Calculate PF angle (θ) of the load by the following equation,

$$\theta = cos^{-1}(PF) \tag{4.5}$$

Step 2: Calculate the reactive power (Q_L) of the load by the following equation,

$$Q_L = S * sin(\theta) \tag{4.6}$$

Step 3: Calculate the desired phase angle ($\emptyset_D$) between the voltage and current waveform of the load by the following equation if the desired PF is to be 0.98 lagging after the compensation,

$$\emptyset_D = \cos^{-1}(0.98) \tag{4.7}$$

Step 4: Calculate the amount of reactive power (Q_{COMP}) for the desired PF of the load by the following equation,

$$\mathrm{Q}_{COMP} = P * \tan(\emptyset_D) \tag{4.8}$$

Step 5: Calculate the amount of reactive power (Q_{ADDED}) needed to improve the PF of the load by the following equation,

$$\mathrm{Q}_{ADDED} = \mathrm{Q}_{\mathrm{D}} - \mathrm{Q}_{COMP} \tag{4.9}$$

Step 6: Calculate the capacitance (C) or inductance (L) required to be connected in parallel with the load by the following equation,

$$C = \frac{Q_{ADDED}}{2\pi * f * V^2} \tag{4.10}$$

$$L = \frac{V^2}{2\pi * f * Q_{ADDED}} \tag{4.11}$$

where, f is the system frequency and V is the rms load voltage.

The flow diagram of the algorithm used in the proposed aromatic PF correction system is shown in Figure 4.12. After the system is started the voltage and current of the load are measured at the beginning. The voltage and current values are reduced to suitable values for the microcontroller using the voltage transformer and current transformer. In this sense, the Arduino Mega 2560 controller has three inputs; voltage, current, and the time delay between the voltage and the current waveform of the load. Then, using the proposed algorithm, the value of the initial PF is calculated before the optimization of the parameters. The electrical parameters of the load, such as, rms voltage, rms current, PF, PF type, real, reactive as well as apparent power of the load are displayed anytime (before or after compensation) on the LCD. After determining the type of the load through the algorithm, Arduino Mega 2560 microcontroller calculates the value of the required capacitors or inductor banks to be connected to the load in parallel to improve the PF. Finally, if the load is lagging, the required capacitor(s) is/are connected in parallel with the load. If the load is leading, the required inductor(s) is/are connected in parallel with the load. If the load is unity, then no action for compensation is made. After PF correction the load, the electrical parameters of the load mentioned before can be observed on the LCD.

Arduino Mega 2560 microcontroller is programed in the following steps:

Step-1: Read voltage, current, and calculate the time delay associated with the phase angle difference.

Step-2: Calculate the PF of the load.

Step-3: Specify the type of the load (unity, lagging, leading)

Step-4: Calculate the inductance(s) or capacitor(s) required to improve the PF of the load close to 0.98 lagging.

Step-5: Generate signals to switch ON the respective relay to connect the desired capacitor(s) or inductor(s) to the load.

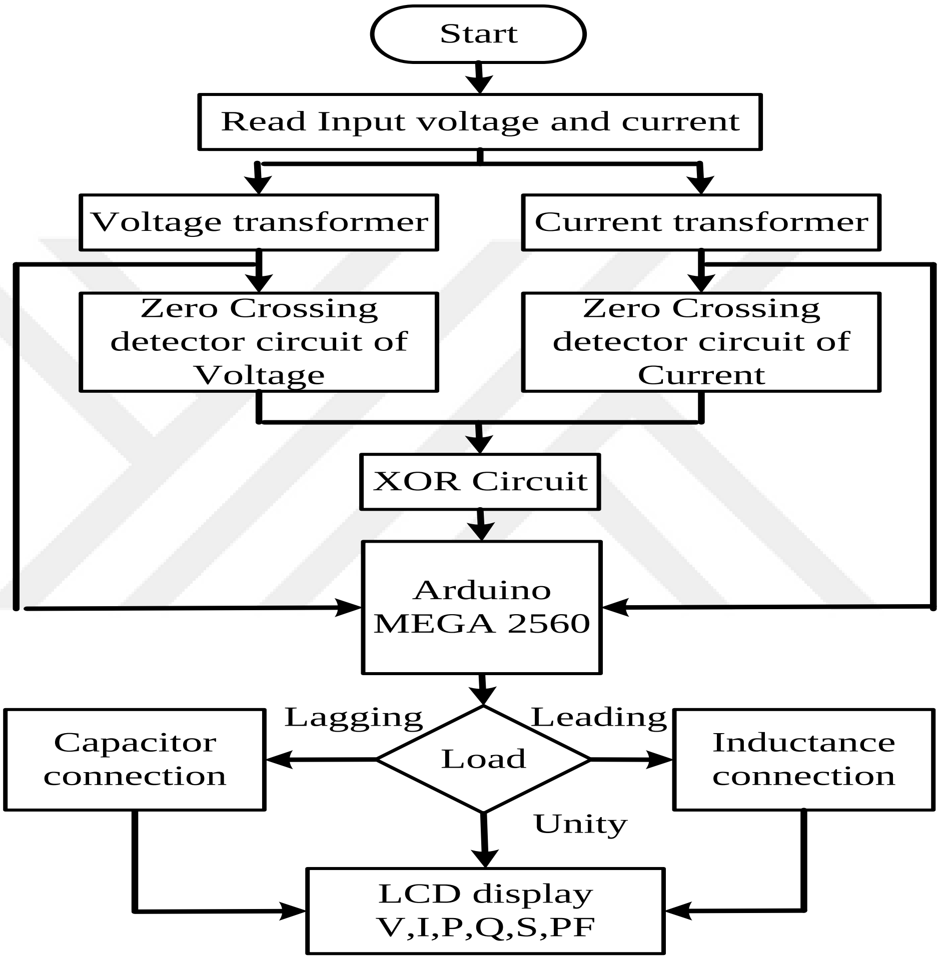

Figure 4.12 The flow diagram of the algorithm.

CHAPTER 5

EXPERIMENT RESULTS

In this study, three different load types are used. These are resistive load, inductive load, and capacitive load. The resistive load is only used to verify the measurements of the electrical parameters of the load handled by the proposed APFC system. Since the proposed APFC system is able to decide how many capacitor or inductor is/are connected to the load in any size, two different load sizes (small and big) are considered in the experiments in order to verify this ability of the proposed system. The measurements taken by the proposed system are verified with a commercial digital power meter (Reed R5000). The measurement error for each electrical parameter of the load is calculated by the following equation,

$$\% \, error = \frac{PM - MC}{PM} \qquad (5.1)$$

where, PM is the power meter reading and MC is the calculated value by the proposed system. It is aimed to obtain this percentage error as small as possible, i.e., less than 10% max. When comparing the measurements taken by the proposed system with the power meter measurements, a maximum percentage error of 8 % is obtained for all load types.

5.1 Case-1 (Resistive Load)

In this case study, two resistive loads (small and big) are considered as shown in Figure 5.1 and 5.2, respectively. The purpose of this case study is to verify the measurement performance of the proposed system. The small resistive load is an incandescent light bulb with a power rating of 100W. On the other hand, the big resistive load is the combination of these two light bulbs with a total power rating of 200W. Both loads operate at 220V rms. Table 5.1 and 5.2 shows the measurements taken by Arduino Mega 2560 microcontroller and the commercial digital power meter for small resistive load and big resistive load, respectively. The measured data of the resistive load is the rms voltage, rms current, PF, active, reactive, and apparent power. The percentage error for each measured data is also represented in Table 5.1 by comparing the measurements taken by Arduino Mega 2560 microcontroller with the digital power meter.

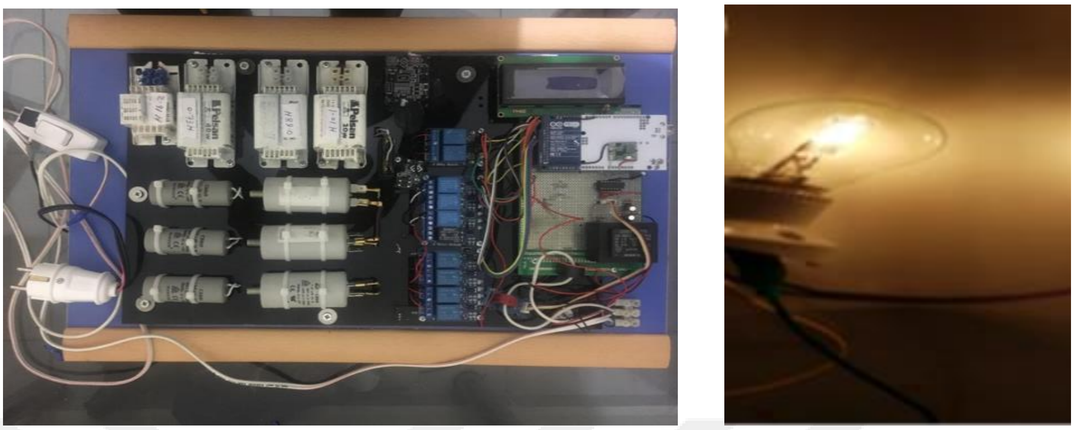

Figure 5.1 Small resistive load.

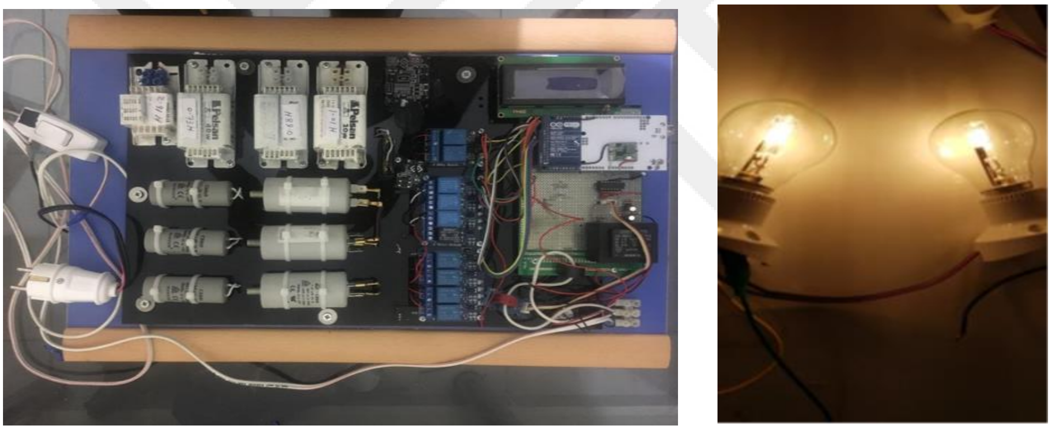

Figure 5.2 Big resistive load

Table 5.1 Measurement results for small resistive load.

Load type: Small Resistive Load				
APF system	***Value***	***Digital power meter***	***Value***	***% error***
Load voltage (V)	228.66	Load voltage (V)	230.4	0.75
Load current (A)	0.42	Load current (A)	0.43	2.32
Load PF	1.00	Load PF	1.00	0

Load type: Small Resistive Load				
APF system	*Value*	*Digital power meter*	*Value*	*% error*
Load active power (W)	95.33	Load active power (W)	99	3.70
Load reactive power (VAR)	3.58	Load reactive power (VAR)	3.77	5.03
Load apparent power (VA)	95.40	Load apparent power	99.072	3.70

Table 5.2 Measurement results for big resistive load.

Load type: Big Resistive Load				
APF system	*Value*	*Digital power meter*	*Value*	*% error*
Load voltage (V)	227.83	Load voltage (V)	230	0.94
Load current (A)	0.81	Load current (A)	0.87	6.89
Load PF	1.00	Load PF	1.00	0
Load active power (W)	185.52	Load active power (W)	200	7.24
Load reactive power (VAR)	6.47	Load reactive power (VAR)	6.32	2.37
Load apparent power (VA)	185.63	Load apparent power (VA)	200.1	7.23

For this case study, the error for the voltage measurements for both loads remains less than 1.0%. On the other hand, the error for current and power measurements for both cases are within 2-7%. It can be concluded that the proposed APFC system measures the electrical parameters of the resistive load with an error of maximum 7.2%.

5.2 Case-2 (Inductive Load)

In this case study, two different inductive loads (small and big) are used as shown in Figure 5.3 and 5.4, respectively. The small load is a single-phase AC motor with a rating of 220V, 50Hz, 43W. The big load is a single-phase AC motor with a rating of 220V, 50Hz, 110W. In this experimental case, both the measurement as well as the compensation performance of the proposed APFC system are verified for lagging PF loads. Table 5.3 shows the measurements taken by the microcontroller and the digital power meter before/after compensation for the small load. The error for the voltage measurements before/after compensation is less than 1.0%. The error for the current measurements before/after compensation is obtained as maximum 7.69%. On the other hand, the errors for the power measurements before/after compensation stay between 1-8%. When the compensation function is activated, the APFC system connects one $2.5uF$ capacitor to the load in parallel to improve the PF from 0.6 to 0.99 lagging. It is deduced that the proposed APFC works well in increasing the PF of the 43W rated single-phase AC motor.

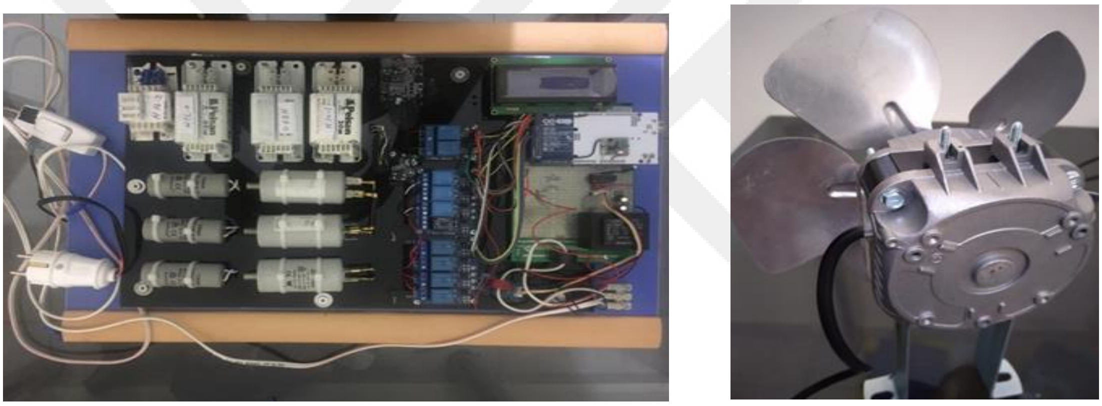

Figure 5.3 Small inductive load.

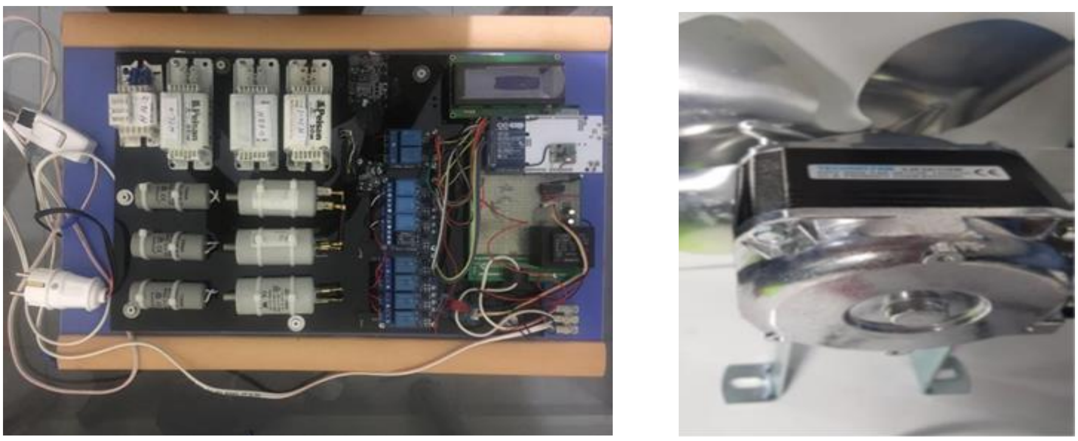

Figure 5.4 Big inductive load.

Table 5.3 Measurement results for small inductive load.

Load type: Small Inductive Load				
APF system (before compensation)	***Value***	***Digital power meter (before compensation)***	***Value***	***% error***
Load voltage (V)	228.27	Load voltage (V)	229.9	0.70
Load current (A)	0.21	Load current (A)	0.21	0
Load PF	0.60	Load PF	0.61	1.63
Load active power (W)	29.62	Load active power (W)	29	2.13
Load reactive power (VAR)	39.26	Load reactive power (VAR)	38.58	1.76
Load apparent power (VA)	49.18	Load apparent power (VA)	48.27	1.88
Load type: Small Inductive Load				
APF system (after compensation)	***Value***	***Digital power meter (after compensation)***	***Value***	***% error***
Load voltage (V)	228.9	Load voltage (V)	230	0.47
Load current (A)	0.14	Load current (A)	0.13	7.69
Load PF	0.99	Load PF	0.97	2.06
Load active power (W)	31.30	Load active power (W)	29	7.93
Load reactive power (VAR)	7.16	Load reactive power (VAR)	7.28	1.64
Load apparent power (VA)	32.11	Load apparent power (VA)	29.9	7.39

Table 5.4 shows the measurements taken by the microcontroller and the digital power meter before/after compensation for the big load. The voltage errors stay again less than 1.0% before/after compensation. The errors for the current measurements before/after compensation remain around 3-4%. On the other hand, the errors for the

power measurements before/after compensation are within 2-7%. When the compensation function is activated, the APFC system connects three capacitors with capacitances of $0.5uF, 1.5uF, and\ 5uF$ to improve the PF from 0.45 to 0.97 lagging. In this case study, it is verified that the measurements taken from the APFC system has a maximum error rate of 7.93% and the PFs of the inductive loads with different sizes are effectively increased to close to unity.

Table 5.4 Measurement results for big inductive load.

Load type: Big Inductive Load				
APF system (before compensation)	***Value***	***Digital power meter (before compensation)***	***Value***	***% error***
Load voltage (V)	230.8	Load voltage (V)	231.5	0.30
Load current (A)	0.62	Load current (A)	0.65	4.61
Load PF	0.45	Load PF	0.47	4.25
Load active power (W)	64.69	Load active power (W)	70	7.58
Load reactive power (VAR)	129.49	Load reactive power (VAR)	133.19	2.77
Load apparent power (VA)	144.75	Load apparent power (VA)	150.47	3.80
Load type: Big Inductive Load				
APF system (after compensation)	***Value***	***Digital power meter (after compensation)***	***Value***	***% error***
Load voltage (V)	228.45	Load voltage (V)	229.9	0.63
Load current (A)	0.31	Load current (A)	0.32	3.21
Load PF	0.97	Load PF	0.97	0
Load active power (W)	69.28	Load active power (W)	71	2.42
Load reactive power (VAR)	17.26	Load reactive power (VAR)	18.37	6.04

Load type: Big Inductive Load				
APF system (before compensation)	***Value***	***Digital power meter (before compensation)***	***Value***	***% error***
Load apparent power (VA)	71.39	Load apparent power (VA)	73.34	2.65

5.3 Case-3 (Capacitive Load)

In this case, two different capacitive loads are used as shown in Figure 5.5 and 5.6, respectively. The small load consists of a 470 Ω resistor connected in series with a 10 uF capacitor. The big load consists of a 235 Ω resistor connected in series with a 12uF capacitor. In this experimental case, both the measurement as well as the compensation performance of the proposed APFC system are verified for leading PF loads. Table 5.5 shows the measurements taken by the microcontroller and the digital power meter before/after compensation for the small load. The error for the voltage measurements before/after compensation is maximum 1.17%. The error for the current measurements before/after compensation is obtained as maximum 2.70%. On the other hand, the errors for the power measurements before/after compensation stay between 0.75-7.35%. When the compensation function is activated, the APFC system connects one 2.91H inductor to the load in parallel to improve the PF from 0.85 leading to 0.97 leading. It is deduced that the proposed APFC works well in increasing the PF of the small capacitive load.

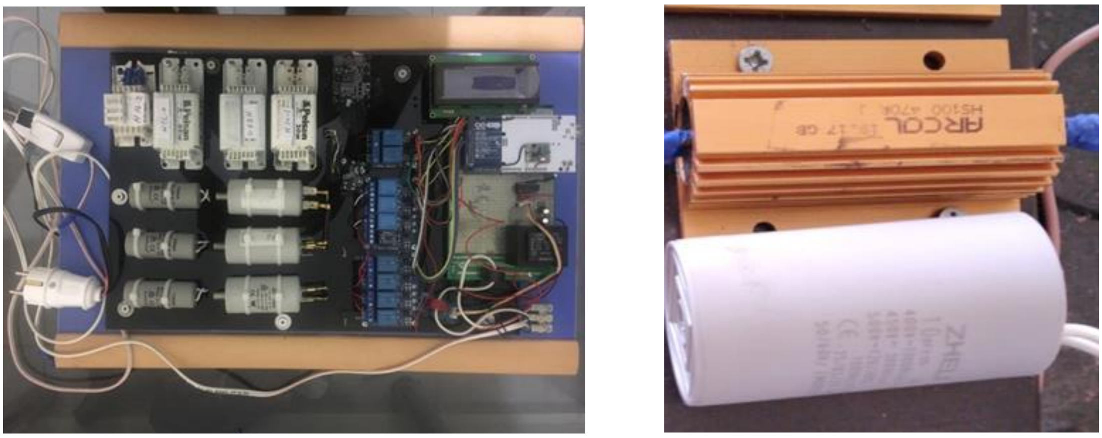

Figure 5.5 Small capacitive load.

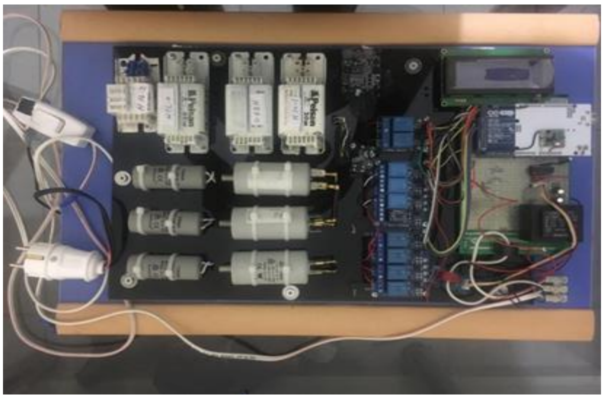

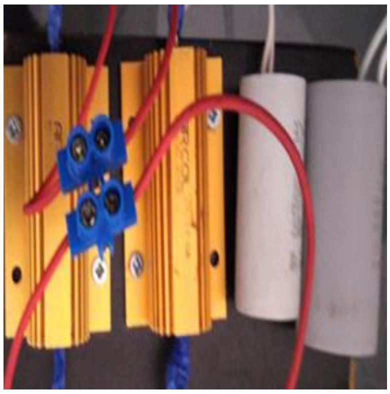

Figure 5.6 Big capacitive load.

Table 5.5 Measurement results for small capacitive load.

Load type: Small Capacitive Load				
APF system (before compensation)	***Value***	***Digital power meter (before compensation)***	***Value***	***% error***
Load voltage (V)	227.61	Load voltage (V)	228.8	0.52
Load current (A)	0.39	Load current (A)	0.39	0
Load PF	0.85	Load PF	0.85	0
Load active power (W)	75.12	Load active power (W)	77	2.44
Load reactive power (VAR)	46.91	Load reactive power (VAR)	45.09	4.03
Load apparent power (VA)	88.56	Load apparent power (VA)	89.232	0.75
Load type: Small Capacitive Load				
APF system (after compensation)	***Value***	***Digital power meter (after compensation)***	***Value***	***% error***
Load voltage (V)	227	Load voltage (V)	229.7	1.17
Load current (A)	0.36	Load current (A)	0.37	2.70

Load type: Small Capacitive Load				
APF system (before compensation)	***Value***	***Digital power meter (before compensation)***	***Value***	***% error***
Load PF	0.97	Load PF	1.00	3
Load active power (W)	78.98	Load active power (W)	84	5.97
Load reactive power (VAR)	13.87	Load reactive power (VAR)	12.92	7.35
Load apparent power (VA)	80.19	Load apparent power (VA)	84.989	5.64

Table 5.6 shows the measurements taken by the microcontroller and the commercial digital power meter before/after compensation for the big load. The maximum voltage measurement error is 1.08% before/after compensation. The errors for the current measurements before/after compensation remain around 3.17-3.92%. On the other hand, the errors for the power measurements before/after compensation are within 3.49-7.74%. When the compensation function is activated, the APFC system connects one inductance 1.01H to the load to improve the PF from 0.68 leading to 0.97 leading. In this case study, it is verified that the measurements taken from the APFC system has a maximum error rate of 7.74% and the PFs of the capacitive loads with different sizes are effectively increased to close to unity.

Table 5.6 Measurement results for big capacitive load.

Load type: Big Capacitive Load				
APF system (before compensation)	***Value***	***Digital power meter (before compensation)***	***Value***	***% error***
Load voltage (V)	228.51	Load voltage (V)	229.9	0.60
Load current (A)	0.61	Load current (A)	0.63	3.17
Load PF	0.68	Load PF	0.68	0

Load type: Big Capacitive Load				
APF system (before compensation)	***Value***	***Digital power meter (before compensation)***	***Value***	***% error***
Load active power (W)	95.22	Load active power (W)	99	3.81
Load reactive power (VAR)	102.02	Load reactive power (VAR)	105.71	3.49
Load apparent power (VA)	139.55	Load apparent power (VA)	144.83	3.64
Load type: Big Capacitive Load				
APF system (after compensation)	***Value***	***Digital power meter (after compensation)***	***Value***	***% error***
Load voltage (V)	228.4	Load voltage (V)	230.9	1.08
Load current (A)	0.49	Load current (A)	0.51	3.92
Load PF	0.97	Load PF	0.99	2.02
Load active power (W)	108.87	Load active power (W)	116	6.14
Load reactive power (VAR)	21.84	Load reactive power (VAR)	20.27	7.74
Load apparent power (VA)	111.04	Load apparent power (VA)	117.759	5.70

CHAPTER 6

CONCLUSIONS

6.1 Conclusions

An automatic power factor correction system was proposed and implemented in this study. This system is able to correct the power factor of both lagging and leading single-phase loads. No matter about the load size, the proposed system can calculate the required number of capacitors or inductors to be connected in parallel. The proposed system can also calculate and display many electrical parameters of the load. From the experimental studies the following points are concluded:

1. The proposed system can get an accurate measurement for PF, voltage, current, Active power, reactive power, and apparent power when validated with the power meter.
2. The proposed system can improve the value of the PF for lagging and leading load by adding a capacitor or inductor in parallel with the load.
3. Arduino microcontroller can successfully calculate the capacitor or inductance required to improve the PF in different load (lagging and leading) with different level (small and big) load
4. The improvement in PF based on the level of load were 39% for small inductive load, 52% for high inductive load, 12% for low capacitive load, and 29% for a high capacitive load.
5. Arduino microcontroller showed high performance in terms of calculate power factor and the required value of capacitor or inductance to improve power factor in both of load (lagging and leading).

REFERENCES

[1] Mane, S., Sapat, R., Kor, P., Shelar, J., Kulkarni, R. D., Mundkar, J. (2020). Microcontroller based Automatic Power Factor Correction System for Power Quality Improvement. *2020 International Conference for Emerging Technology (INCET)* 1-6. IEEE.

[2] Uddin, M. M., Al Mahmud, A., Islam, N. (2019). Design & Implementation of a Microcontroller Based Automatic Power Factor Rectification System for Different Loads. *2019 1st International Conference on Advances in Science, Engineering and Robotics Technology* (*ICASERT*) 1-6 IEEE.

[3] Zaky, M. S., Azazi, H. Z., Touti, E. (2018). PFC Control for LED Lamp Driver Using Sensorless Predictive Current Controller. *Engineering, Technology & Applied Science Research*, **8(5),** 3373-3379.

[4] Tsolov, A., Marinova, B. (2018). Optimal Power Factor for the Reactive Load of Small Hydro Power Plants. *Engineering, Technology & Applied Science Research*, **8**, 2755-2757.

[5] Kayabaşi, A., Akkaya, R. (2009). The Design and Implementation of a Microcontroller-Based Single Phase On-line Uninterrupted Power Supply with power Factor Correction. *2009 International Conference on Electrical and Electronics Engineering-ELECO 2009* I-442 IEEE.

[6] Sehwag, V., Dua, V., Singh, A., Rai, J. N., Shekhar, V. (2018). Power Factor Correction Using APFC Panel on Different Loads. *2018 2nd IEEE International Conference on Power Electronics, Intelligent Control and Energy Systems* (*ICPEICES*) 73-77 IEEE.

[7] Ali, W., Farooq, H., Jamil, M., Rehman, A. U., Taimoor, R., Ahmad, M. (2018). Automatic Power Factor Correction for Single Phase Domestic Loads by Means

of Arduino Based TRIAC Control of Capacitor Banks. *2018 2nd International Conference on Energy Conservation and Efficiency* (*ICECE*) 72-76 IEEE.

[8] Jarad, S. B., Lohar, V. D., Choukate, S. P., Mangate, S. D. (2018). Automatic Optimization and Control of Power Factor, Reactive Power and Reduction of THD for Linear and Nonlinear Load by Using Arduino UNO. *2018 Second International Conference on Inventive Communication and Computational Technologies (ICICCT)* 1128-1132 IEEE.

[9] Adiningtyas, G., Lestari, N. S., Triwiyatno, A., Warsito, A. (2019). An Automatic Single Phase Power Factor Compensator using Fuzzy and Gain Scheduling. 2019 *IEEE Conference on Energy Conversion (CENCON)* 12-17 IEEE.

[10] Qiao, X., Bian, J., Chen, C., Li, H. (2019). Comparison and Analysis of Reactive Power Compensation Strategy in Power System. *2019 IEEE Sustainable Power and Energy Conference (iSPEC)* 689-692 IEEE.

[11] Zheng, F., Zhang, W. (2017). Long Term Effect of Power Factor Correction on the Industrial Load: A case study. *2017 Australasian Universities Power Engineering Conference (AUPEC)* 1-5 IEEE.

[12] Qin, W., Wang, P., Han, X., Du, X. (2010). Reactive power aspects in reliability assessment of power systems. IEEE Transactions on Power Systems, **26**(**1**), 85-92.

[13] Shaker, A. M., Ismail, K. S., Salih, A. M. (2008). Design and Simulation of Power Factor Correction for AC/DC Converter. Journal of Engineering, **14**(**2**), 2591-2605.

[14] Choudhury, S. M. (2008). Design and Implementation of a Low Cost Power Factor Improvement Device. In TENCON 2008-2008 IEEE Region 10 Conference (pp. 1-4). IEEE.

[15] Afridi, M. N. (2012). Design and Implementation of Automatic Microcontroller-Based Controlling of Single Phase Power Factor Using Capacitor Banks with Load Monitoring. Global Journal of Research in Engineering, **12**(10-F).

[16] Biswas, R. S., Mal, S. (2015). Automatic Power Factor Improvement Using Microcontroller. *2015 International Conference and Workshop on Computing and Communication (IEMCON)* 1-6 IEEE.

[17] Sayed, R., Ferdous, A. H. M. I., Shobug, M. A. (2015). Automatic Power Factor Correction by Using Synchronous Condenser with Continuous Monitoring. Int. J. Elect. Comput. Syst, **4**(**5**), 12-17.

[18] Utpal, Rishav, Tiwari, M. (2016). Automatic Power Factor Correction Using Capacitor Banks. International Journal of Innovative Research in Electrical, Electronics, Instrumentation and Control Engineering. **4**(**4**), 9-16.

[19] Taye, A. (2018). Design and Simulation of Automatic Power Factor Correction for Industry Application. International Journal of Engineering Technologies and Management Research, **5** (**4**) 10-21.

[20] Ranjan, R., Kumar, D., Anand, A., Namekar, S. (2017). Automatic Power Factor Correction Using Microcontroller. International Research Journal of Engineering and Technology(IRJET), **4**(**6**).

[21] Ahmed, M. R., Kabir Khan, M. H., Karmaker, A. K. (2018). Microcontroller - based Power Factor Improvement Using Switched Single Capacitor. DUET Journal, **4**(**1**), 21-28.

[22] Stet, D., Czumbil, L., Micu, D. D., Polycarpou, A., Ceclan, A., Cretu, M. (2019). Power Factor Correction Using EMTP-RV for Engineering Education. *2019 54th International Universities Power Engineering Conference (UPEC)* 1-5. IEEE.

[23] Ehsan, M. T., Anwar, A., Ahsan, F., Rehman, M. A. U., Kamran, M. (2019). Pic Microcontroller based power factor correction for both leading and lagging loads using compensation method. *2019 16th International Bhurban Conference on Applied Sciences and Technology (IBCAST*) 377-383 IEEE.

[24] Jumah Al-Thahab, O. Q., hasoony, A. S., Alkhafaji, A. S. (2020). Sixteen Level Power Factor Correction by Using Arduino Microcontroller Based Fuzzy Idea.

Indonesian Journal of Electrical Engineering and Computer Science, **17**(**1**), 156-165.

[25] Maklakov, A. S., Radionov, A. A., Gasiyarov, V. R. (2016). Power Factor Correction and Minimization THD in Industrial Grid Via Reversible Medium Voltage AC Drives Based on 3L-NPC AFE Rectifiers. In *IECON 2016-42nd Annual Conference of the IEEE Industrial Electronics Society* (pp. 2551-2556). IEEE.

[26] Mansouri, M., Kaboli, S. H. A., Selvaraj, J., Rahim, N. A. (2013). A Review of Single Phase Power Factor Correction AC-DC Converters. *2013 IEEE Conference on Clean Energy and Technology (CEAT)* 389-394 IEEE.

[27] Marcos-Pastor, A., Vidal-Idiarte, E., Cid-Pastor, A., Martinez-Salamero, L. (2015). Interleaved Digital Power Factor Correction Based on The Sliding-Mode Approach. IEEE Transactions on Power Electronics, **31** (**6**) 4641-4653.

[28] Marouani, K., Nounou, K., Benbouzid, M., Tabbache, B. (2014). Power factor correction of an electrical drive system based on multiphase machines. *2014 First International Conference on Green Energy ICGE 2014* , 152-157 IEEE.

[29] Moury, S., Lam, J., Srivastava, V., Church, R. (2016). A Novel Multi-Input Converter Using Soft-Switched Single-Switch Input Modules with Integrated Power Factor Correction Capability for Hybrid Renewable Energy Systems. *2016 IEEE Applied Power Electronics Conference and Exposition (APEC)* 786-793 IEEE.

[30] Ravindran, M., Kirubakaran, V. (2012). Electrical Energy Conservation in Automatic Power Factor Correction by Embedded System. Energy and Power, **2**(**4**), 51-54.

[31] Grey, A. D. (2005). Power Factor Improvement Using Fuzzy Logic Control of an AC Synchronous Motor. In Proceedings. IEEE SoutheastCon, 2005. 193-199 IEEE.

[32] Coman, C. M., Florescu, A., Oancea, C. D. (2020). Improving the Efficiency and Sustainability of Power Systems Using Distributed Power Factor Correction Methods. Sustainability, **12**(**8**), 3134.

[33] Hashmi, M. U., Deka, D., Busic, A., Pereira, L., Backhaus, S. (2020). Arbitrage with Power Factor Correction Using Energy Storage. IEEE Transactions on Power Systems.

[34] Alberts, J. A., De Kock, J. A. (2017). Impact on Power Factor by Small Scale Renewable Energy Generation. *2017 International Conference on the Domestic Use of Energy (DUE)* 146-151 IEEE.

[35] Benyamina, A., Moulahoum, S. (2019). FPGA in The Loop Based Single Phase Power Factor Correction. *2019 Progress in Applied Electrical Engineering (PAEE)* 1-6 IEEE.

[36] Chandra, A., Singh, B., Singh, B. N., Al-Haddad, K. (2000). An Improved Control Algorithm of Shunt Active Filter for Voltage Regulation, Harmonic Elimination, Power-Factor Correction, and Balancing of Nonlinear Loads. IEEE transactions on Power electronics, **15**(**3**), pp. 495-507.

[37] Chen, J., Zhang, X., Wen, C. (2016). Harmonics attenuation and power factor correction of a more electric aircraft power grid using active power filter. IEEE Transactions on Industrial Electronics, **63**(**12)**, pp. 7310-7319.

[38] de Castro, A., Zumel, P., García, O., Riesgo, T., Uceda, J. (2003). Concurrent and Simple Digital Controller of an AC/DC Converter with Power Factor Correction Based on an FPGA. IEEE Transactions on Power Electronics, **18**(1), pp. 334-343.

[39] Gatta, F. M., Geri, A., Maccioni, M., Mantineo, A., Cresta, M., Paulucci, M. (2015). Reactive Power Control Strategy for Voltage Regulation and Power-Factor Correction in MV Distribution Networks. In 2015 IEEE Eindhoven PowerTech (pp. 1-6). IEEE.

[40] González-Santini, N. S., Zeng, H., Yu, Y., Peng, F. Z. (2016). Z-Source Resonant Converter with Power Factor Correction for Wireless Power

Transfer Applications. IEEE Transactions on Power Electronics, **31**(**11**), pp. 7691-7700

[41] Wang, L., Liu, K. H. (2004). Improvement of Power Factor and Voltage for Renewable Energy Systems Using PLC's New Fuzzy Module. *2004 IEEE Asia-Pacific Conference on Circuits and Systems, 2004. Proceedings*. **2**, pp. 957-960 IEEE.

[42] Allewar, S. V., Shaha, R. (2018). Simulation of High Performance Utility by Improving Power Factor in PV Grid System. Simulation, **5**(**5**).

[43] Islam, S. R., Maxwell, S., Hossain, M. K., Park, S. Y., Park, S. (2016). Reactive Power Distribution Strategy Using Power Factor Correction Converters for Smart Home Application. *2016 IEEE Energy Conversion Congress and Exposition (ECCE)* 1-6 IEEE.

[44] Zhang, W., Feng, G., Liu, Y. F., Wu, B. (2004). A Digital Power Factor Correction (PFC) Control Strategy Optimized for DSP. IEEE Transactions on Power Electronics, **19**(**6**), pp. 1474-1485.

[45] Duddell, W. (1901). On the Resistance and Electromotive Forces of the Electric ARC. Proceedings of the Royal Society of London, **68**(442-450), 512-518.

[46] Zhang, S. (2006). Analysis of Some Measurement Issues in Bushing Power Factor Tests in the Field. IEEE Transactions on Power Delivery, **21**(**3**), 1350-1356.

[47] Almarshoud, A. F., Abdel-Halim, M. A., Alolah, A. I. (2004). Performance of Grid-Connected Induction Generator Under Naturally Commutated AC Voltage Controller. Electric Power Components and Systems, **32**(**7**), 691-700.

[48] Ohyama, T., Watanabe, A., Nishimura, K., Tsuruta, S. (1985). Voltage Dependence of Composite Loads in Power Systems. IEEE Transactions on Power Apparatus and Systems, (**11**), 3064-3073.

[49] Kundur, P., Balu, N. J., Lauby, M. G. (1994). Power System Stability and Control (Vol. **7**). New York: McGraw-hill.

[50] Kambli, M. N. A. (2017). Automatic Power Factor Detector and Correction Using Arduino UNO (Doctoral dissertation, University OF Mumbai).

[51] Theraja, B. L., Theraja, A. K. (2005). A text Book of Electrical Technology, **2** AC and DC machines .

[52] Irwin, J. D., Nelms, R. M. (2015). Basic Engineering Circuit Analysis. Wiley.

[53] Nikum, K., Wagh, A. (2020). Hadware Implementation of Step-Switched SVCs to Correct Power factor and Mitigate Harmonics for Large DC Variable Loads. Journal of The Institution of Engineers (India): Series B, 1-13.

[54] Ali, F., Arbab, M. N., Ahmad, G., Ashraf, M., Sarim, M. (2020). An SVC Controller for Power Quality Improvement of a Heavily Loaded Grid. Mehran University Research Journal of Engineering and Technology, **39**(**2**), 247-256.

[55] Soodi, H. A., Vural, A. M. (2018). Single phase nine-level convertor based STATCOM for reactive power compensation and power factor correlation. *2018 International Conference on Engineering Technology and their Applications (IICETA)* 19-24 IEEE.

[56] Soodi, H. A., Vural, A. M. (2018). STATCOM Estimation Using Back-Propagation, PSO, Shuffled Frog Leap Algorithm, and Genetic Algorithm Based Neural Networks. Computational intelligence and neuroscience, 2018.

[57] Vural, A. M. (2012). Modeling of Multi-Converter FACTS (Flexible Alternating Current Transmission Systems) (Doctoral Dissertation, PhD Dissertation, Cukurova University).

[58] Drápela, J., Bok, J. (2008). An improved Valley-Fill Passive Power-Factor-Correction circuit for electronic ballast. *simulation*, **60**, (**80**).

[59] Carbone, R. (2009). A passive power factor correction technique for single-phase thyristor-based controlled rectifiers. International Journal of Circuits, Systems and Signal Processing, (**2**), 169-179.

[60] Azazi, H. Z., El-Kholy, E. E., Mahmoud, S. A., Shokralla, S. S. (2010). Review of passive and active circuits for power factor correction in single phase, low power AC-DC converters. In Proceedings of the 14th International Middle East Power Systems Conference (MEPCON'10) (p. 217-224).

[61] Kumar, P. (2008). Development of Power Factor Controller Using PIC Microcontroller (Doctoral dissertation).

[62] Soodi, H. A., Vural, A. M. (2019). Controller Parameter Optimization for a 13-Level Cascaded H-Bridge Medium Voltage Static Synchronous Compensator. International Transactions on Electrical Energy Systems, **29**(**4**), e2805.

[63] Tun, M. Z., Swe, P. L. (2014). Power Factor Correction with Synchronous Motor for Rice Mill. International Journal of Scientific Engineering and Technology Research, **3**, 1-5.

[64] Bayindir, R., Colak, I., Kabalci, E., Gorgun, A. (2009). PID controlled synchronous motor for power factor correction. *2009 International Conference on Power Engineering, Energy and Electrical Drives* 408-412 IEEE.

[65] Routray, S. S. (2015). Microcontroller Based Automatic Power Factor Correction in Mines (Doctoral dissertation).

[66] Hadzhiev, I., Malamov, D., Balabozov, I., & Yatchev, I. (2020). Study of Operational Parameters of a Capacitor Bank with Detuned Reactor for Power Factor Correction in a Low Voltage Network. *2020 21st International Symposium on Electrical Apparatus & Technologies (SIELA)* 1-4 IEEE.

[67] Gumilar, L., Cahyani, D. E., & Sholeh, M. (2020). Combination Detuned Reactor and C-Type Filter for Electrical Power System under Harmonic Condition. *2020 7th International Conference on Information Technology, Computer, and Electrical Engineering (ICITACEE)* 219-223 IEEE.

[68] No Title Https://www.arduino.cc/en/uploads/Tutorial/pwm.gif

[69] Lee, R. M. (1993). U.S. Patent No. **5**,245,220. Washington, DC: U.S. Patent and Trademark Office.

APPENDIX

SOFTWARE CODE

```
#include "configuration.h"

void setup()

{

  V_I_MONITOR.voltage(v_sensor, 175, 0.8);

  V_I_MONITOR.current(i_sensor, 2);

  Serial.begin(9600);

  lcd.begin(20, 4);

  pinMode(18, OUTPUT);//LED LCD

  digitalWrite(18, HIGH);

  delay(500);

  for (int i = 0; i <= 4; i++) {

    pinMode(C_BANK_PINS[i], OUTPUT);

    digitalWrite(C_BANK_PINS[i], HIGH);

    pinMode(L_BANK_PINS[i], OUTPUT);

    digitalWrite(L_BANK_PINS[i], HIGH);

  }

  pinMode(Status, INPUT);
```

```
  pinMode(v_sensor, INPUT_PULLUP);
  pinMode(i_sensor, INPUT_PULLUP);
  pinMode(shift_pulse, INPUT_PULLUP);
  Serial.println("START");
  delay(5000);
  attachInterrupt(digitalPinToInterrupt(v_pulse), PF_ISR, RISING);
  delay(1000);
  lcd.begin(20, 4);
  lcd.clear();
  lcd.setCursor(4, 1);
  lcd.print("APFC SYSTEM");
  delay(1000);
  lcd.clear();
  lcd.setCursor(0, 0);
  lcd.print("PF      =");
  lcd.print(PF_Type);
  delay(1000);
}
void loop()
```

```
{

  V_I_MONITOR.calcVI(20, 2000);
  float supplyVoltage   = V_I_MONITOR.Vrms;
  float loadcurrent     = V_I_MONITOR.Irms;
  if (supplyVoltage > 50) {
    V_I_MONITOR.serialprint();
    V_I_angle = phase_shifte();
    P = abs(supplyVoltage * loadcurrent * PF);
    S = supplyVoltage * loadcurrent;
    Q = sqrt(pow(S, 2) - pow(P, 2));
    Serial.print("P="); Serial.print(P); Serial.println("Watte");
    Serial.print("Q="); Serial.print(Q); Serial.println("VAR");
    Serial.print("S="); Serial.print(S); Serial.println("VA");
    /////////////////////////**************
    lcd.clear();
    lcd.setCursor(0, 1);
    lcd.print("before correction...");
    delay(2000);
```

```
lcd.clear();

lcd.setCursor(0, 0);

lcd.print("Vin=  "); lcd.print(supplyVoltage); lcd.print("  "); lcd.print("I=  "); lcd.print(loadcurrent);

delay(2000);

lcd.clear();

lcd.setCursor(0, 0);

lcd.print("PF=  "); lcd.print(PF); lcd.print("    "); lcd.print("Angle=  "); lcd.print(V_I_angle);

lcd.setCursor(0, 1);

lcd.print("P= "); lcd.print(P); lcd.print(" W");

lcd.setCursor(0, 2);

lcd.print("Q= "); lcd.print(Q); lcd.print(" VAR");

lcd.setCursor(0, 3);

lcd.print("S= "); lcd.print(S); lcd.print(" VA");

delay(3000);

if (PF_Type == "lag") {

  float C_target = PF_COR(P , supplyVoltage, V_I_angle * 0.017444);



  if (C_target >= 0) {
```

```
      lcd.clear();

      lcd.setCursor(0, 1);



    }

    Update_PF(C_target);

  }

  if (PF_Type == "lead") {

    float L_target = PF_COR(P , supplyVoltage, V_I_angle * 0.017444);



    lcd.clear();

    lcd.setCursor(0, 1);



    Update_PF(L_target);



  }

  while (1) {

  }



}
```

```
}

void PF_ISR() {
  if (digitalRead(i_pulse) == 0) {
    PF_Type = "lag";

  }
  else {
    PF_Type = "lead";

  }
  detachInterrupt(digitalPinToInterrupt(v_pulse));
  Serial.print("PF=            ");
  Serial.println(PF_Type);

  delay(1000);
}

void Active_CAP(float target) {
```

```
float result = 0.0;

int n_target = target / 0.5;
float N_target = n_target  * 0.5;
if (target - N_target > 0) {
  target = N_target + 0.5;
}
else {
  target = N_target;
}

if (target >= 0.5 && target <= 10) {
  lcd.setCursor(0, 2);
  lcd.print("C_con= "); lcd.print(target); lcd.print(" uF");
}
for (int i = 0; i < 32; i++) {
  result = result + (i & 1) * C_BANK_VALUES[0];
  result = result + ((i & 2) / 2) * C_BANK_VALUES[1];
```

```
    result = result + ((i & 4) / 4) * C_BANK_VALUES[2];

    result = result + ((i & 8) / 8) * C_BANK_VALUES[3];

    result = result + ((i & 16) / 16) * C_BANK_VALUES[4];

    Serial.println(result);

    if (result == target) {

      int c_scan = 1;

      for (int c = 0; c < 5; c++) {

        digitalWrite(C_BANK_PINS[c], !((i & c_scan) / c_scan));

        c_scan = c_scan * 2;

      }

       digitalWrite(C_BANK_PINS[4], !((i & 16) / 16));*/

      result = 0;

      break;

    }

    else {

    }

    result = 0;

  }

}
```

```
void Active_IND(float target) {

  float result = 0.0;
  float min_L = 10;
  int ind_L = 0;

  for (int i = 0; i <= 15; i++) {
    result = 0;
    result = result + (i & 1) * L_BANK_VALUES[0];
    result = result + ((i & 2) / 2) * L_BANK_VALUES[1];
    result = result + ((i & 4) / 4) * L_BANK_VALUES[2];
    result = result + ((i & 8) / 8) * L_BANK_VALUES[3];
    result = 1 / result;

    if (min_L > (target - result) && (target - result) >= 0) {
      ind_L = i;
      min_L = target - result;
      Serial.print("i=");   Serial.print(i);   Serial.print("    ");   Serial.print("===>");
Serial.println(min_L);
```

```
    }
    result = 0;

  }

  int l_scan = 1;
  for (int l = 0; l < 4; l++) {
    digitalWrite(L_BANK_PINS[l], !((ind_L & l_scan) / l_scan));
    l_scan = l_scan * 2;
  }
  if (target >= 0.24 && target <= 2.6) {

  }
  lcd.setCursor(0, 2);
  lcd.print("L_con= "); lcd.print(target - min_L); lcd.print(" H");

  result = 0;
}
```

```
float PF_COR(int Pw , int Vin, float Ang1) {
  int S1; int Q1; int Q2; int Qc_l; float C_L; float L; float Ang2 = acos(0.99);
  lcd.clear();

  if (PF_Type == "lag") {
    S1 = Pw / cos(Ang1); Serial.print("S1="); Serial.println(S1);
    Q1 = S1 * sin(Ang1); Serial.print("Q1="); Serial.println(Q1);
    Q2 = Pw * tan(Ang2); Serial.print("Q2"); Serial.println(Q2);
    Qc_l = Q1 - Q2; Serial.print("Qc_l="); Serial.println(Qc_l);
    C_L = Qc_l * 1000000 / (2 * PI * F * pow(Vin, 2));/*value in uf*/
Serial.print("C="); Serial.print(C_L); Serial.print("uF");
  }
  if (PF_Type == "lead") {
    S1 = Pw / cos(Ang1); Serial.print("S1="); Serial.println(S1);
    Q1 = S1 * sin(Ang1); Serial.print("Q1="); Serial.println(Q1);
    Q2 = Pw * tan(Ang2); Serial.print("Q2"); Serial.println(Q2);
    Qc_l = -Q1 - Q2; Serial.print("Qc_l="); Serial.println(Qc_l);
    C_L = (pow(Vin, 2)) / (2 * PI * F * Qc_l);/*value in H*/Serial.print("L=");
Serial.print(C_L); Serial.print("H");
    C_L = abs(C_L);
```

```
  }
  return C_L;
}

float phase_shifte() {
  V_I_angle = 0;
  for (int i = 0; i <= 99; i++)
  {
    duration = pulseIn(shift_pulse, HIGH);
    V_I_angle += ((duration * nano * degree * frequency);
  }
  V_I_angle = abs(V_I_angle / 100);
  PF = cos(V_I_angle * 0.017444);
  Serial.print("angle=");    Serial.print(V_I_angle);    Serial.print("<<->>"); Serial.print("PF="); Serial.println(PF);
  return V_I_angle;
}

void Update_PF(float C_L_Value) {
  Serial.print("APFC start");
```

```
if (PF_Type == "lag")
  Active_CAP(C_L_Value);
if (PF_Type == "lead")
  Active_IND(C_L_Value);
delay(5000);
V_I_MONITOR.voltage(v_sensor, 175, 0.8);
V_I_MONITOR.current(i_sensor, 2);
V_I_MONITOR.calcVI(20, 2000);
V_I_MONITOR.serialprint();
float supplyVoltage   = V_I_MONITOR.Vrms;
float loadcurrent     = V_I_MONITOR.Irms;
V_I_angle = phase_shifte();
P = abs(supplyVoltage * loadcurrent * PF);
S = supplyVoltage * loadcurrent;
Q = sqrt(pow(S, 2) - pow(P, 2));
lcd.clear();
lcd.setCursor(1, 1);
lcd.print("After correction...");
delay(2000);
```

```
  lcd.clear();

  lcd.setCursor(0, 0);

  lcd.print("Vin=  "); lcd.print(supplyVoltage); lcd.print("  "); lcd.print("I=  ");
lcd.print(loadcurrent);

  delay(2000);

  lcd.clear();

  lcd.setCursor(0, 0);

  lcd.print("PF=  "); lcd.print(PF); lcd.print("     "); lcd.print("Angle=  ");
lcd.print(V_I_angle);

  lcd.setCursor(0, 1);

  lcd.print("P= "); lcd.print(P); lcd.print(" W");

  lcd.setCursor(0, 2);

  lcd.print("Q= "); lcd.print(Q); lcd.print(" VAR");

  lcd.setCursor(0, 3);

  lcd.print("S= "); lcd.print(S); lcd.print(" VA");

}
```